Journal of Chromatography A 1638 (2021) 461857

Contents lists available at ScienceDirect

Journal of Chromatography A

journal homepage: www.elsevier.com/locate/chroma

# Preparation of value-added metal-organic frameworks for high-performance liquid chromatography. Towards green chromatographic columns

Ahmad Aqel[a,*], Norah Alkatheri[a], Ayman Ghfar[b], Ameen M. Alsubhi[a], Zeid A. ALOthman[a,b], Ahmed-Yacine Badjah-Hadj-Ahmed[a,*]

[a] Department of Chemistry, College of Science, King Saud University, Riyadh, Saudi Arabia
[b] Advanced Materials Research Chair, Department of Chemistry, College of Science, King Saud University, Riyadh, Saudi Arabia

ARTICLE INFO

*Article history:*
Received 1 November 2020
Revised 20 December 2020
Accepted 26 December 2020
Available online 29 December 2020

*Keywords:*
Metal-organic framework
MIL-53(Al)
Green chromatography
Polyethylene terephthalate bottles
Column preparation
Stationary phase

ABSTRACT

This work applies the concepts of green chemistry, where polyethylene terephthalate (PET) bottles were used as the acid-dicarboxylic linker source for the synthesis of MIL-53(Al) metal organic frameworks (MOFs) and then used as a stationary phase for the separation of various solutes and compared with MIL-53(Al) synthesized from traditional terephthalic acid. Both synthesized MIL-53(Al) MOFs were characterized by scanning electron microscopy (SEM), FT-IR, X-ray diffraction (XRD), thermogravimetric analysis (TGA), and specific surface area analysis. Eight groups of standard analytes in addition to real samples were tested to evaluate the separation performance of the MIL-53(Al) packed columns in HPLC under various chromatographic conditions. Based on elution order of the studied compounds and the effects of mobile phase composition, the working mechanism was reversed phase mode in the presence of size-exclusion effects for large molecules, which exceeded the dynamic diameter of MIL-53(Al) (~7.6 Å). The effects of stationary phase sieving, mobile phase flow rate and composition, injected sample mass, and temperature were investigated relative to the chromatographic behavior of MIL-53(Al). MIL-53(Al) particle sieving before packing reduced peak broadening and significantly enhanced the chromatographic performance of the prepared columns up to 2.26 times relative to the number of theoretical plates. The MIL-53(Al) packed columns offered high-resolution separation for all studied mixtures with $R_s$ >2 and good stability and long-term durability. At optimal conditions, the prepared columns exhibited efficiencies between 5600−63200 plates $m^{-1}$. Higher efficiencies were observed for alkylbenzenes and polyaromatic hydrocarbons as the organic linker in the MIL-53(Al) structure, which improved retention and separation of aromatics through $\pi-\pi$ interactions. Thermodynamic parameters including $\Delta H$, $\Delta S$, and $\Delta G$ for the transfer of analyte from the mobile phase to the MIL-53(Al) stationary phase were studied. Compared with previously cited MOFs packed columns, the present MIL-53(Al) columns gave comparable selectivity and much better efficiency for most of the studied chemicals at optimum conditions, indicating the feasibility of MIL-53(Al) as a stationary phase for HPLC applications.



## 1. Introduction

Over the last two decades, metal-organic frameworks (MOFs) have attracted great attention from researchers working in various fields of sciences such as physics, chemistry, engineering, material science, and others. MOFs are a class of porous solid materials constructed from inorganic metal ions and organic functional linkers [1,2]. The interesting physical and chemical properties, along with the pore topologies of MOF structures, provide tremendous diversity, and the ability to rationally tune the end products, leading to a wide range of promising applications in gas storage [3], separation [4], catalysis [5], sample preparation [6], chemical sensing [7], biomedicine [8], drug delivery [9], food safety [10], imaging [11], water harvesting [12], and so on [1,13].

Due to the advantageous properties of MOFs, such as large surface area, uniform, and tunable pore size, high thermal stability, and semi-organic pore walls, MOFs have been regarded as ideal materials to be used as adsorbents and stationary phases in chromatography [4,14–19]. Several classical MOFs, such as HKUST-1, MOF-5, DUT-67(Zr), MIL-53(Al/Fe), MIL-125(Ti), MIL-47(V), MIL-100(Fe), MIL-101(Cr), ZIF-8, and UiO-66(Zr) have been

* Corresponding Author.
*E-mail address:* aifseisi@ksu.edu.sa (A. Aqel).

https://doi.org/10.1016/j.chroma.2020.461857
0021-9673/

used as stationary phases for HPLC separation to analyze chemical compounds [14–19]. The major drawbacks of traditional MOFs used as stationary phases in liquid chromatography applications are the low column efficiency, noticeable peak broadening, and high pressure drops due to the significant variation in most MOF particle sizes and their irregular, non-spherical shapes [15]. However, to enhance the chromatographic performance of MOFs-based materials, some groups have tried to prepare MOF-composites with silica [20], organic polymer monoliths [21], or graphene [22]. In all reports, MOFs were either physically incorporated or chemically linked to the added materials to provide further interactions to the composite material and improve separation performance [14–22]. These composites were applied as stationary media, combining the preferred properties of both materials into one to increase the separation ability of the MOFs. Herein, we took advantage of sieving the prepared materials as a simple and cheap method to obtain a much narrower particle size range, which was able to improve the stationary phase distribution inside the column and enhance the efficiency of the packed columns.

Plenty of porous coordination networks have been prepared via several techniques, but the hydrothermal/solvothermal approach is one of the most popular methods for the synthesis of MOF materials [23]. Traditionally, MOF materials are prepared by the reaction of metal ions with commercially available or presynthesized linkers. Via careful selection of their constituents, MOFs can meet the attributes necessary for successful separations. As a good stationary phase, the material should have an adequate surface area, as required for analyte retention and suitable separation, as well as uniform particle size and shape which help to reduce peak broadening and enhance column efficiency. Also, this candidate material should have excellent chemical stability and a high mechanical resistance. However, the diversity of organic linkers and metal centers, and the availability of various synthesis and modification strategies open up a wide array of possibilities for the preparation of MOFs suitable for the separation of a wide range of samples.

The MIL-*n* family (MIL; stands for Material Institute Lavoisier) is a subclass of MOFs associated with Férey's group [24]. Generally, MILs are based on a trivalent cation, such as $Al^{3+}$, $Fe^{3+}$, $Ga^{3+}$, $In^{3+}$, or $Cr^{3+}$, and an organic ligand of di-, tri-, or tetracarboxylic acid that can form linear diamond-shaped networks. Due to high surface area, good chemical and water stability, remarkable adsorption affinities, and the presence of uniform pores that allow for the inclusion of small molecules, MIL-53 type MOFs are one of the most promising as adsorbents or stationary phases for liquid chromatography [4,14–22]. MIL-53(Al) was first prepared by mixing aluminum nitrate and terephthalic acid (TPA) in the presence of water at 220°C for 72 h [25].

Today, materials chemistry and analytical techniques tend to develop green and cheaper approaches to reduce costs and minimize environmental impacts. Polyethylene terephthalate (PET) has been widely used in food and beverage packaging since the 1960s [26]. PET is a clear and lightweight polymer with good chemical resistance and mechanical strength and high gas and odor barrier properties. PET is commonly prepared by the esterification of TPA and ethylene glycol; it is mainly used to manufacture transparent plastic bottles around the globe [27]. Increased consumption of PET, and hence, increased PET waste, has caused serious environmental problems due to the polymer's high resistance to degradation [28]. However, valuable amounts of high purity TPA can be recycled from PET bottle waste [28–30]. Since TPA is the main starting compound for the synthesis of several types of MOFs, the development of a successful method to extract TPA from PET waste would offer an environmentally and economically attractive approach to produce a value-added material by recycling waste PET. Based on a similar strategy, other MOFs have been successfully prepared, such as MIL-101(Cr), MIL-47, MIL-53(Cr, Al, Ga), and UiO-66(Zr) [28,30,31]. To the best of our knowledge, no studies on the application of such a scenario have been attempted in the field of chromatography and even adsorption so far.

Herein, the present work aims to use PET waste material as a source of TPA for the preparation of MIL-53(Al) as a way to contribute to green chemistry concepts. This value-added material was then used as a stationary phase in HPLC. For comparison with the prepared MOF, MIL-53(Al) was also synthesized from a commercial TPA reagent. Both synthesized MIL-53(Al) materials were characterized by scanning electron microscopy (SEM), FT-IR, X-ray diffraction (XRD), thermogravimetric analysis (TGA), and specific surface area analysis. Eight groups of analytes containing polar, neutral, non-polar, acidic, and basic compounds, in addition to green tea water extract, were tested to evaluate the separation performance of the MIL-53(Al) packed column in HPLC, under various chromatographic conditions. The separation mechanism on the stationary phase was also investigated. The influence of the stationary phase particle size, mobile phase composition and flow rate, injected sample mass, and temperature were also explored with respect to the chromatographic behavior of MIL-53(Al). Several thermodynamic parameters including $\Delta H$, $\Delta S$, and $\Delta G$ for the transfer of analyte from the mobile phase to the MIL-53(Al) stationary phase were also studied. Finally, the main findings were compared to other previous reports in terms of chromatographic parameters and separation performance.

## 2. Experimental

### 2.1. Chemicals and reagents

Aluminum nitrate nonahydrate, TPA, hydrofluoric acid, formic acid, ethanol, benzene, toluene, *n*-ethylbenzene, *n*-propylbenzene, *n*-butylbenzene, *n*-pentylbenzene, 1-phenylhexane, *m*-xylene, *p*-xylene, *o*-xylene, mesitylene, naphthalene, indene, acenaphthylene, fluorene, anthracene, phenanthrene, pyrene, chrysene, butyrophenone, acetophenone, phenol, resorcinol, phloroglucinol, 4-aminophenol, 4-chlorophenol, 4-nitrophenol, *p*-cresol, 2-naphthol, theobromine, theophylline, and caffeine were purchased from Acros Organics (Morris County, NJ, USA), BDH (Lutterworth, UK), and Sigma-Aldrich (St. Louis, MO, USA). PET bottles were collected from local waste. HPLC grade acetonitrile (ACN) and acetone were acquired from Fisher Scientific (Leicestershire, UK). Ultrapure water was prepared using a Millipore Elix Advantage, Milli-Q system (Molsheim, France), and then filtered on 0.20 $\mu$m nylon membrane filters from Whatman (Maidstone, UK). A green tea sample was obtained from a local supermarket (Riyadh, Saudi Arabia) as a powder (tea bag; 2.0 g) and stored in vacuum packaging at a temperature below 0°C.

### 2.2. Synthesis of MIL-53(Al)

Using our green approach, the PET bottle material was used as the starting precursor, instead of TPA, for the synthesis of MIL-53(Al). Waste PET water bottles were cut into small pieces. MIL-53(Al) was synthesized according to the procedure described by Lo et al. [31]. In a typical procedure, $Al(NO_3)_3 \bullet 9H_2O$ (375 mg, 1.0 mmol) and PET flakes (192 mg) were mixed with ultrapure water (4.0 mL, 222 mmol) in a Teflon-lined stainless-steel autoclave reactor, then placed in an oven and heated at 160°C for 72 hours. The autoclave was cooled to room temperature, the resulting mixture was filtered, and the unreacted PET was removed by hand picking and solid filtration. The final product was washed with water and dried in a vacuum oven at 100°C overnight prior to packing. This procedure was repeated to collect the desired quantity of MIL-53(Al) powders. The schematic representation of the synthetic

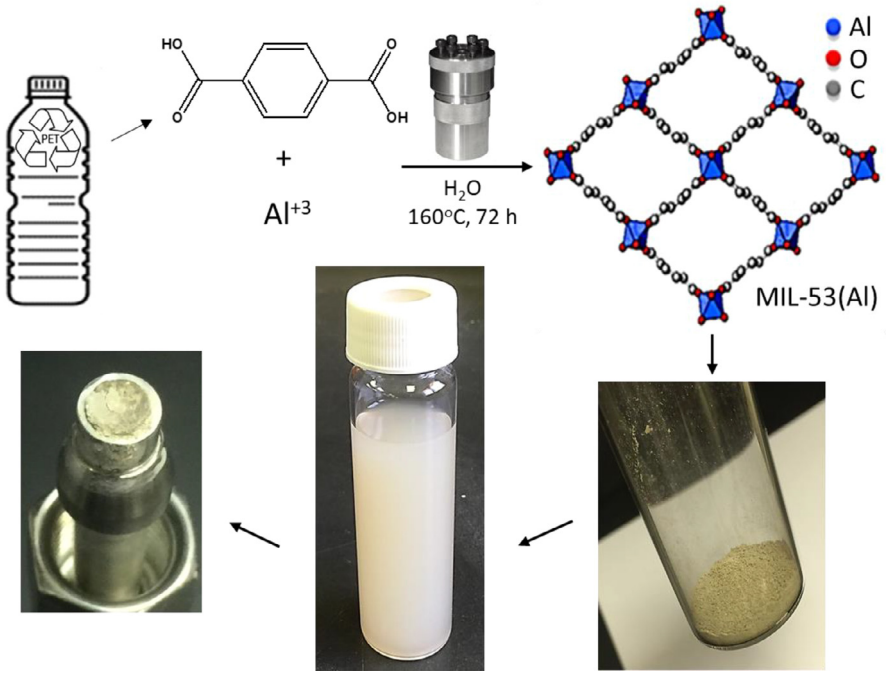


**Fig. 1.** Representation of the synthesis procedure and the porous framework structural representation of MIL-53(Al). The obtained MIL-53(Al) powder, the suspension of MOF powders in ethanol, and photograph of the prepared column.

procedure, the structural framework representation, and the obtained gray crystalline powder of MIL-53(Al) are shown in Fig. 1.

For comparison, MIL-53(Al) was also synthesized from commercial TPA (Sigma-Aldrich) according to a method suggested in a previous study performed by Loiseau et al. [25] as follows: 1.30 g of $Al(NO_3)_3 \bullet 9H_2O$ and 0.288 g of TPA were mixed in a Teflon-lined stainless-steel autoclave with 5.0 mL water, and then placed in an oven and heated at 220°C for 72 hours. The autoclave was cooled to room temperature; the product was filtered, washed with water, and dried in a vacuum oven at 100°C overnight prior to packing.

### 2.3. Columns preparation

To obtain a uniform particle size range of solid packing used as stationary phase, the synthesized MIL-53(Al) was sieved between 5 $\mu$m (sieve no. L3-M5) and 10 $\mu$m (sieve no. L3-M10) sieves using an Advantech Sonic Sifter Separator L3P-25 (New Berlin, WI, USA). 1.5 g of the sieved powders were ultrasonically dispersed in a suitable vessel (Fig. 1) with 25 mL of absolute ethanol for 10 min. The suspension was slurry packed into stainless-steel columns (50, 100, and 150 mm long × 4.6 mm i.d.) and subjected to 5000 psi (about 34.5 MPa) pressure for 30 min using a Restek packing station (Bellefonte, PA, USA). Stainless-steel frits with a pore size of 0.5 $\mu$m were placed at both ends to ensure MIL-53(Al) stayed in the column. The prepared columns were conditioned with HPLC grade ACN at a flow rate of 0.10 mL $min^{-1}$ for 3 h before chromatographic experiments.

### 2.4. Instrumentation and columns characterization

All chromatographic experiments were carried out using a Shimadzu (Kyoto, Japan) HPLC system consisting of a LC-20AD quaternary pump, a SIL-20A auto sampler, a CTO-20A column oven, a SPD-M20A diode array detector, and a DGU-20A5R degasser. Shimadzu's LC Lab Solution software was used to control the system and acquire and process chromatographic data.

SEM images of the synthesized MIL-53(Al) were obtained using a Jeol JSM-7500F (Tokyo, Japan) scanning electron microscope at 20 kV. The Fourier transform infrared spectroscopy (FT-IR) spectra of the prepared MOFs were recorded on a Thermo Nicolet 6700 FT-IR spectrophotometer (Madison, WI, USA). MOF materials were mixed with KBr, and the spectra were measured in the range of 400–4000 $cm^{-1}$. The XRD patterns were recorded at room temperature with a Bruker D2 Phaser with XFlash detector (Madison, WI, USA) using $CuK_\alpha$ radiation ($\lambda$ = 1.5418 Å) in a range of $2\theta$ = 5–80°. Thermal stabilities of MOFs were measured using TGA with a Mettler-Toledo TGA/DSC Stare system (Schwerzenbach, Switzerland). The samples were heated from room temperature to 1100°C at a ramp rate of 10°C $min^{-1}$. The Brunauer-Emmett-Teller (BET) technique was used to obtain the surface area of the prepared MOFs using a Gemini VII 2390 Micromeritics surface area analyzer (Norcross, GA, USA) at 77 K. The synthesized MOFs were ground and degassed at 200°C before data acquisition.

### 2.5. Chromatographic and thermodynamic parameters

To investigate the efficiency of the prepared columns, a wide range of standard compounds were tested as model solutes: alkylbenzenes, PAHs, ketones, phenols, xylenes, and methylxanthines. The effects of the analyte mass, mobile phase flow rate, column temperature, and composition of the mobile phase were evaluated. Various chromatographic parameters including retention time ($t_R$), width at half peak ($w_{0.5}$), number of theoretical plates ($N$), retention factor ($k$), selectivity factor ($\alpha$), resolution between neighboring peaks ($R_s$), and asymmetry factor ($A_s$) were studied in all cases. The injection volume was fixed at 5 $\mu$L.

The enthalpy change ($\Delta H$), entropy change ($\Delta S$), and Gibbs free energy change ($\Delta G$) for the analyte transfer from the mobile phase to the MIL-53(Al) stationary phase were calculated from the van't Hoff and Gibbs free energy equations [32,33]:

$$\ln k = \frac{-\Delta H}{RT} + \frac{\Delta S}{R} \ln \Phi \quad (1)$$

$$\Delta G = \Delta H - T\Delta S \quad (2)$$

where $R$ is the ideal gas constant (8.314 J $mol^{-1}$ $K^{-1}$), $T$ is the absolute temperature, and $\Phi$ is the phase ratio. The void time ($t_0$) of the columns used for $k$ value calculation was determined by injecting a small amount of ACN and recording the repeatable perturbation signal.

## 3. Results and discussion

### 3.1. Characterization of the synthesized MIL-53(Al)

MIL-53(Al) was obtained by heating a mixture of 375 mg of $Al(NO_3)_3 \bullet 9H_2O$, 192 mg of a waste PET bottle, and 4.0 mL of water. In this green preparation approach, waste PET water bottles were recycled and used as the ligand source instead of the pure TPA. The weakest chemical bond in the PET chain is the ester link (C–O bond). Therefore, less energy is needed to break this bond and thus, PET depolymerization mostly occurs by breaking this bond [34,35], and TPA and ethylene glycol are produced. After cooling the reaction vessel, the obtained yellowish gray crystalline powder was collected, as shown in Fig. 1. Since the particles of un-reacted amorphous PET had relatively larger sizes than that of crystalline MIL-53(Al) powder, the two solid phases were easily separated by hand picking and solid filtration. The yield of this reaction did not exceed 44% relative to MIL-53(Al) (based on the unreacted PET). Doubling the amounts of starting materials did not provide a higher amount of product; however, the procedure was repeated to collect the desired quantity of MOFs.

After synthesis and purification, the synthesized MIL-53(Al) was characterized by SEM (Figs. 2A & 2B), FT-IR (Figs. 2C & 2D), XRD (Figs. 2E & 2F), TGA (Figs. 2G & 2H), and specific surface area analysis. Comparatively, MIL-53(Al) prepared using TPA was also subjected to the same investigations. The morphology of MIL-53(Al) prepared by the green approach (Fig. 2A) and the regular procedure (Fig. 2B) were compared with SEM micrographs. The obtained results indicate that MIL-53(Al) has irregular shapes with a broad particle size distribution in the range 2.17–26.8 $\mu$m for MIL-53(Al) prepared by both methods. These results are comparable to those previously cited in literature [31,36]. The FT-IR spectra of MIL-53(Al) prepared by the green method (Fig. 2C) and regular approach (Fig. 2D) were recorded at room temperature in the region of 400–4000 $cm^{-1}$. Peaks in the region of 1400–1700 $cm^{-1}$ illustrate the coordination between the O–C=O carboxylate group and $Al^{3+}$ cation. The strong band at 1580 $cm^{-1}$ can be assigned to the asymmetric stretching of carboxylate groups, whereas the bands at 1445 and 1417 $cm^{-1}$ correspond to the symmetric stretching of carboxylate groups. The sharp band at 1508 $cm^{-1}$ corresponds to the C–C ring vibrations. An additional weak absorption peak in the 1697 $cm^{-1}$ region could be attributed to the stretching vibration of unreacted –COOH groups located within the pores. The low wavenumber vibrations at 468 and 587 $cm^{-1}$ are due to the existence of the Al–O band in MIL-53(Al) [37,38]. A low intensity band at about 3434 $cm^{-1}$ corresponds to bridging OH groups, while the band at 984 $cm^{-1}$ is due to the deformation modes of these bridging hydroxyl groups. As observed in the FTIR spectra, the synthesized MIL-53(Al) from PET water bottles showed a similar characteristic profile to that of MIL-53(Al) prepared by the regular method, both in accordance with literature [25,37–39].

The XRD spectra for MIL-53(Al) prepared from PET water bottles and commercial TPA are presented in Figs. 2E & 2F, respectively. As shown in the figures, there is good agreement between both patterns, which also agrees with literature reports [31,39–41]. The characteristic signals positioned at $2\theta$ = 8.6°, 10.3°, 12.4°, 14.3°, 15.2°, 17.8°, 20.4°, 25.2°, and 26.9° indicate that the MIL-53(Al) crystal structure was successfully synthesized. The sharp XRD peaks between 10 to 40 degrees in both samples indicate the formation of highly and comparable crystallized structures. The thermal stability of the prepared MOFs was evaluated from room temperature to 1000°C, as demonstrated in Fig. 2G (MOF made from PET water bottles) and Fig. 2H (MOF prepared from commercial TPA). Both figures show that the thermal behavior of MIL-53(Al) is characterized by four weight loss regions. The initial weight loss between 25–100°C was assigned to the loss of water molecules from the pores. The gradual weight loss beyond 100°C and up to 500°C may be due to the departure of the free disordered acid. The MIL-53(Al) framework starts to decompose around 500°C; this corresponds to the elimination of the TPA linker from the framework. Above 640°C, MIL-53(Al) is transformed into amorphous $Al_2O_3$. This observed high decomposition temperature suggests that MIL-53(Al) has a robust structure. TGA profiles for MIL-53(Al) materials synthesized by both methods are quite similar and comparable to those reported in previous works [25,39,40,42]. Further interesting characteristics of the prepared MOFs were revealed by surface area analysis using the BET technique. The specific surface area of MIL-53(Al) synthesized from PET water bottles and commercial TPA MIL-53(Al) were 952 and 1141 $m^2$ $g^{-1}$ respectively. The large specific surface area of the final product can provide more interaction sites and contact areas; this feature confirms the attractive and promising applications of this material as a stationary phase. The measured BET surface area values were comparable to previously reported results [25,36,39,40,42].

### 3.2. Column preparation and evaluation

Several research groups have described the preparation of various MOFs and their applications as the stationary phase in HPLC [32,33,43–63]. However, the low efficiency of the columns packed with MOFs could likely result from their wide range of particle sizes and irregular shapes. In the present work, to maintain uniform stationary phase packing, more consistent shapes, and a narrow particle size distribution inside the column, the synthesized MIL-53(Al) powders were sieved prior to packing into the columns. The sieving process was conducted in a nominal range between 5 and 10 µm. 1.5 g of the collected MOFs were dispersed by sonication in 25 mL ethanol for 10 min. The fine powder was well suspended and stable in ethanol, as displayed in Fig. 1. While maintaining a stable suspension, the mixture was immediately poured into empty stainless-steel columns (50, 100, and 150 mm long × 4.6 mm i.d.) and packed under 5000 psi (about 34.5 MPa) for 30 min. Fig. 1 shows a photograph of one of the prepared columns packed with MIL-53(Al). Prior to their evaluation and application, the packed columns were conditioned with ACN at a flow rate of 0.1 mL $min^{-1}$ until a constant column backpressure was observed.

To explore the effects of MIL-53(Al) sieving on column performance, a comparative study was performed between two columns: one packed with MIL-53(Al) as synthesized, and the other after stationary phase sieving. For this purpose, both columns were pushed to their optimum performance for separation of a xylenes mixture. The effect of sieving on the chromatographic behavior of the MIL-53(Al) stationary phase is demonstrated in the Supporting Information (Table S1 and Figs. S1 & S2). While the selectivity factors of the analytes on the two columns were almost the same, all other chromatographic parameters were obviously improved after the sieving process, as presented in Table S1. The shape of the peaks was also affected; the peak width and asymmetry were clearly reduced after MIL-53(Al) particle sieving, as shown in Fig. S1. As a result, higher separation quality and chromatographic resolution were obtained with the column packed with sieved material. The enhancement in the separation efficiency was more than 1.47 times in terms of the number of theoretical plates. Fig. S2A shows the van Deemter plots for *p*-xylene on MIL-53(Al) columns

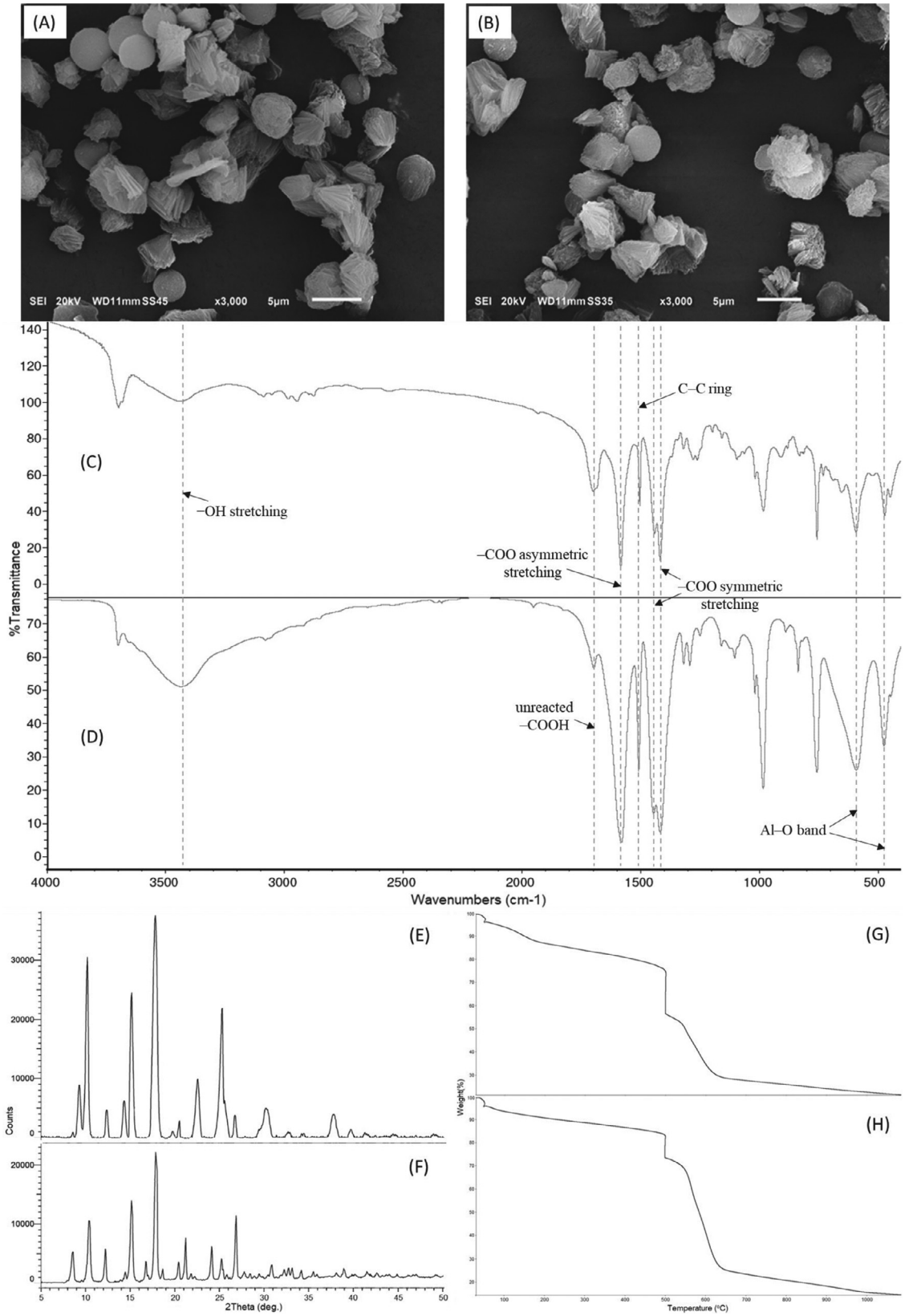


**Fig. 2.** Characterization of synthesized MIL-53(Al). SEM images of MIL-53(Al) prepared by green approach (A) and by regular approach (B). FT-IR spectra of MIL-53(Al) prepared by green approach (C) and by regular approach (D). XRD patterns of MIL-53(Al) powders prepared by green approach (E) and by regular approach (F). TGA curves of the synthesized MIL-53(Al) prepared by green approach (G) and by regular approach (H).

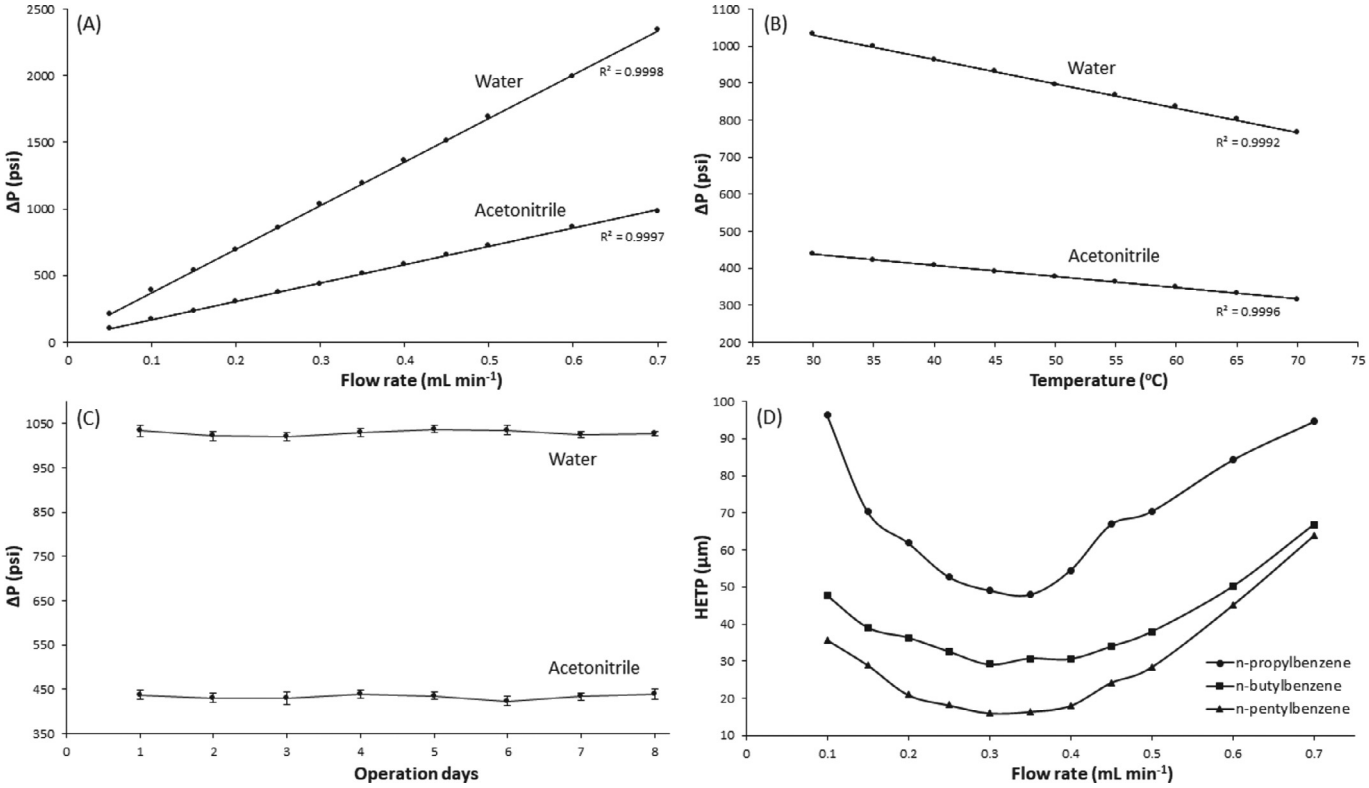


**Fig. 3.** (A) Pressure drop versus flow rate curves of $H_2O$ and ACN as eluents at column temperature 30°C for MIL-53(Al) 100 mm long column prepared from PET water bottles. (B) Pressure drop versus column temperature curves of $H_2O$ and ACN as eluents at a constant flow rate of 0.30 mL $min^{-1}$ for MIL-53(Al) 100 mm long column prepared from PET water bottles. (C) Graph illustrating plots of pressure drop versus operation days as $H_2O$ and ACN passed through the MIL-53(Al) 100 mm long column at 0.30 mL $min^{-1}$ flow rate. (D) Van Deemter plots for some of the studied alkylbenzenes.

before and after sieving. The best efficiency values obtained for *p*-xylene on MIL-53(Al) columns were 3100 plates $m^{-1}$ at 0.30 mL $min^{-1}$ and 7000 plates $m^{-1}$ at 0.35 mL $min^{-1}$, before and after sieving, respectively, which showed a 2.26x increase. On the other hand, the backpressure of the packed column increased by about 1.27% ± 0.03% after sieving due to the lower column permeability and narrower particle size distribution (Fig. S2B). In brief, MIL-53(Al) sieving before packing significantly enhanced the chromatographic performance of the prepared columns.

The stability of the stationary phase is crucial in any HPLC application. The stability of the prepared MIL-53(Al) was investigated in terms of common chromatographic solvents, mobile phase flow rate, pressure, column temperature, operation time, and separation repeatability for replicate injections. ACN and $H_2O$ were eluted through the columns to measure the backpressure at different flow rates ranging from 0.05 to 0.70 mL $min^{-1}$. Fig. 3A shows the relationship between solvent flow rate and column backpressure. In all cases, the backpressure of the column did not exceed 3000 psi (20.7 MPa), which is useful in extending the lifetime of the separation column. As expected, the columns exhibited higher pressure values for water according to the solvent viscosity. On the other hand, the pressure drops of the prepared columns linearly increased over the applied flow rate ranges at a constant column temperature. This linear dependence with regression factors greater than 0.9997 indicate good mechanical stability and permeability for the prepared MIL-53(Al) columns. Further investigation regarding the MIL-53(Al) column stability was carried out with respect to temperature. Fig. 3B reveals that column pressure linearly decreased over a temperature range of 30 to 70°C using ACN and $H_2O$ as eluents at a fixed flow rate of 0.30 mL $min^{-1}$. The backpressure of the column decreased from 438 to 315 psi for ACN, and from 1034 to 765 psi for $H_2O$, corresponding to about 15 ± 2 psi and 33 ± 5 psi per 5° increase, for these two solvents, respectively. The decrease in observed pressure is consistent with the eluent viscosity reduction. The stability of column backpressure against flow rate was also evaluated over eight successive days. The curves in Fig. 3C display an excellent stability of column backpressure (±9 psi) over the operating days at 0.30 mL $min^{-1}$ flow rate, as ACN and $H_2O$ passed through the MIL-53(Al) column at 30°C. In conclusion, the synthesized stationary phase and prepared packed columns did not show significant stability defects resulting from bleeding of the stationary phase or breathing effects of MIL-53(Al) under the applied chromatographic conditions of mobile phase solvents (ACN/$H_2O$), flow rate (0.05–0.70 mL $min^{-1}$), column backpressure (up to 3000 psi), and temperature (25–70°C).

### 3.3. Chromatographic mode and the effect of mobile phase composition

To elucidate the separation mechanism of MIL-53(Al) columns, a variety of analytes including polar, neutral, non-polar, acidic, and basic compounds, were used as model molecules. High-resolution separation of these compounds was achieved on the prepared columns at optimal chromatographic conditions (Figs. 4, 5, & 6). The elution order of most tested solutes indicated a RP-HPLC retention mechanism as on the $C_{18}$ column from the most to the least polar analytes. The xylene mixture (Fig. 4A) was the most important exception. As in NP mode, MIL-53(Al) showed a preference for the retention of *o*-xylene isomer even under RP mode conditions. The stronger retention of *o*-xylene could be explained by the interaction of this highest polarity isomer with the carboxyl and hydroxyl moieties of the MIL-53 framework, which is not predominant for the other xylene isomers [43,44]. However, the same behavior was observed on MIL-101(Cr) [32] and MIL-53(Fe) at 75°C

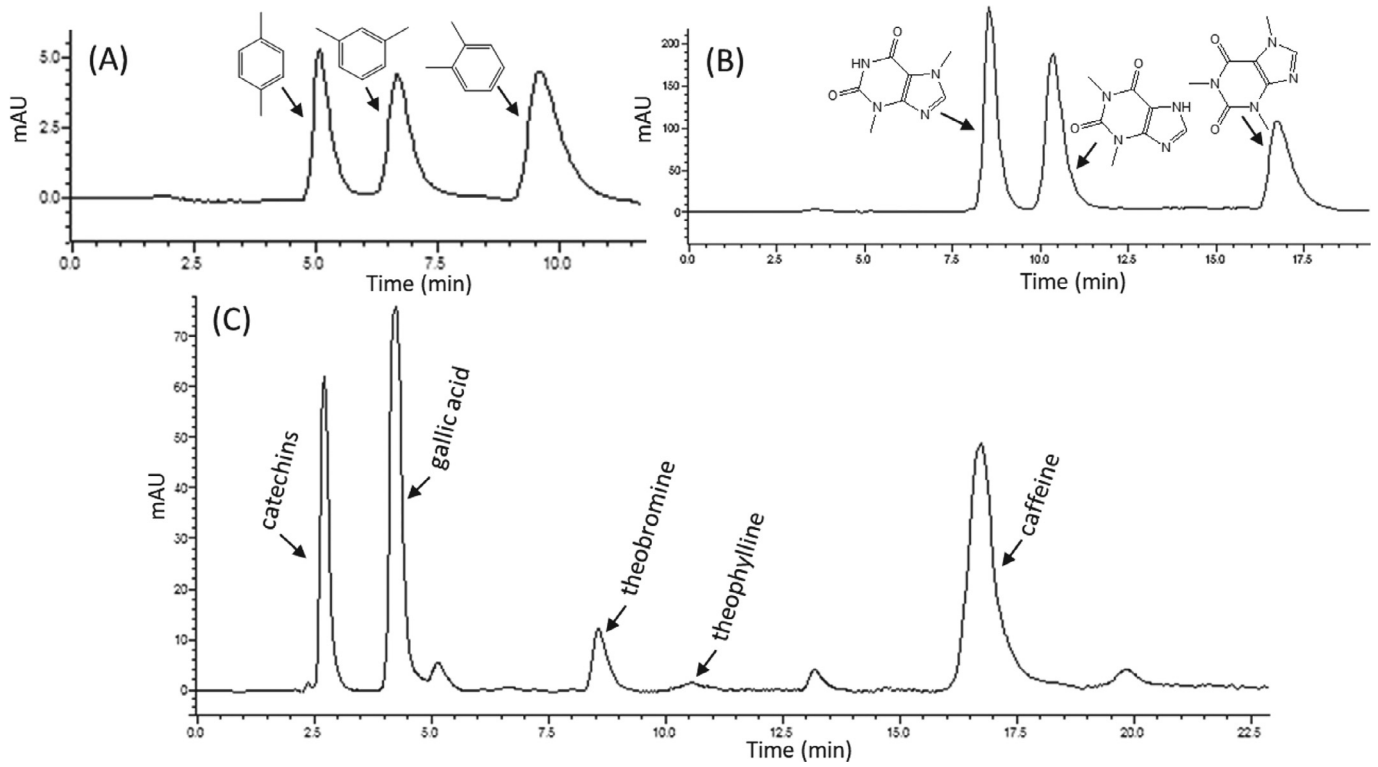


**Fig. 4.** (A) Chromatogram of the separation of xylenes mixture using MIL-53(Al) (150 mm long × 4.6 mm i.d.) column. Conditions: flow rate: 0.35 mL $min^{-1}$, detection wavelength: 254 nm, mobile phase: ACN/$H_2O$ (65:35, v/v), column temperature: 30°C. Peaks by order of elution: (1) *p*-xylene, (2) *m*-xylene, and (3) *o*-xylene. (B) Chromatogram of the separation of methylxanthines mixture using MIL-53(Al) (150 mm long × 4.6 mm i.d.) column. Conditions: flow rate: 0.25 mL $min^{-1}$, detection wavelength: 273 nm, mobile phase: ACN/$H_2O$ (70:30, v/v), column temperature: 30°C. Peaks by order of elution: (1) theobromine, (2) theophylline, and (3) caffeine. (C) Chromatogram of the green tea hot water extract injected at the same conditions as in (B).

column temperature [33]. In contrast, MIL-47 [45] and MIL-100(Fe) [46] stationary phases did not exhibit the same preference.

For the alkylbenzenes mixture (Fig. 5A), the elution order of all compounds was consistent with a reversed-phase mode using ACN/$H_2O$ (70:30, v/v) as the mobile phase. However, an incomplete separation of the first three homologues (benzene, toluene, and ethylbenzene) was obtained at ACN percentages >75%. For PAHs with up to three aromatic rings, such as those shown in Fig. 5B, the elution sequence was in accordance with the hydrophobicity of the compounds which increases with the number of rings. Starting from four aromatic rings (pyrene (Fig. 5B), chrysene, and dibenzo(a,h)anthracene (Supporting Information Figs. S3A & S3B)), the compounds showed lower retention due to size-exclusion effects as their dynamic diameter exceeded 8 Å. Since the dynamic diameter of the MIL-53(Al) at low temperature is about 7.6 Å [25], larger molecules cannot access the pores of MIL-53(Al) efficiently at room temperature. The same behavior was observed for ketonic and phenolic mixtures (Fig. 6), but with lower retentions due to their higher polarity. In conclusion, the results showed that the composition of the mobile phase significantly affected both retention and resolution of all studied analytes on the MIL-53(Al)-prepared columns. Based on the elution order of the studied compounds, the main working mechanism is the RP mode in the presence of size-exclusion effects for large molecules.

To further consolidate the RP separation mode on the MIL-53(Al) columns, the effect of the mobile phase composition was tested using different ratios of ACN/$H_2O$. As an example, Fig. 7 clearly reveals that the separation of the benzene, toluene, *m*-xylene, and mesitylene mixture was remarkably affected by the mobile phase composition. Increasing the polarity of the mobile phase, by lowering its ACN content, leads to increased retention times and improved chromatographic resolution and column efficiency of all molecules. That effect resulted from the enhanced hydrophobic $\pi$-$\pi$ interactions between the analytes and aromatic ring walls of the pores of MIL-53(Al) framework. On the other hand, the order of the studied compounds remained unchanged at all tested mobile phase compositions.

### 3.4. HPLC applications

A variety of analytes (a total of 34 solutes and 8 mixtures) with different chemical and structural properties, including aromatic hydrocarbons, aromatic positional isomers, phenols, ketones, and methylxanthines mixtures, in addition to green tea water extract were injected to evaluate the separation performance of the MIL-53(Al) packed columns in HPLC under various chromatographic conditions. All standards were dissolved and diluted in can, and 5 µL of each mixture was injected into the column. As mentioned in the experimental section, three column dimensions were prepared: 50, 100, and 150 mm long with the same i.d. 4.6 mm. However, the shorter column did not show high enough efficiency for the separation of some of the tested analytes under all examined conditions. As an example, Fig. S3C (Supporting Information) shows the separation chromatogram of the alkylbenzenes using a 50 mm long MIL-53(Al) column. Thus, only the MIL-53(Al) columns prepared inside 100 and 150 mm long stainless-steel tubes were used in all of the next experiments.

#### 3.4.1. HPLC separation of alkylbenzenes and PAHs

A mixture of seven alkylbenzenes was injected to explore the separation performance of the MIL-53(Al) packed column (100 long × 4.6 mm i.d.). Fig. 5A displays the typical separation of alkylbenzenes at 0.30 mL $min^{-1}$ flow rate in about 25 min using ACN/$H_2O$ (60:40, v/v) as the isocratic mobile phase. The chro-

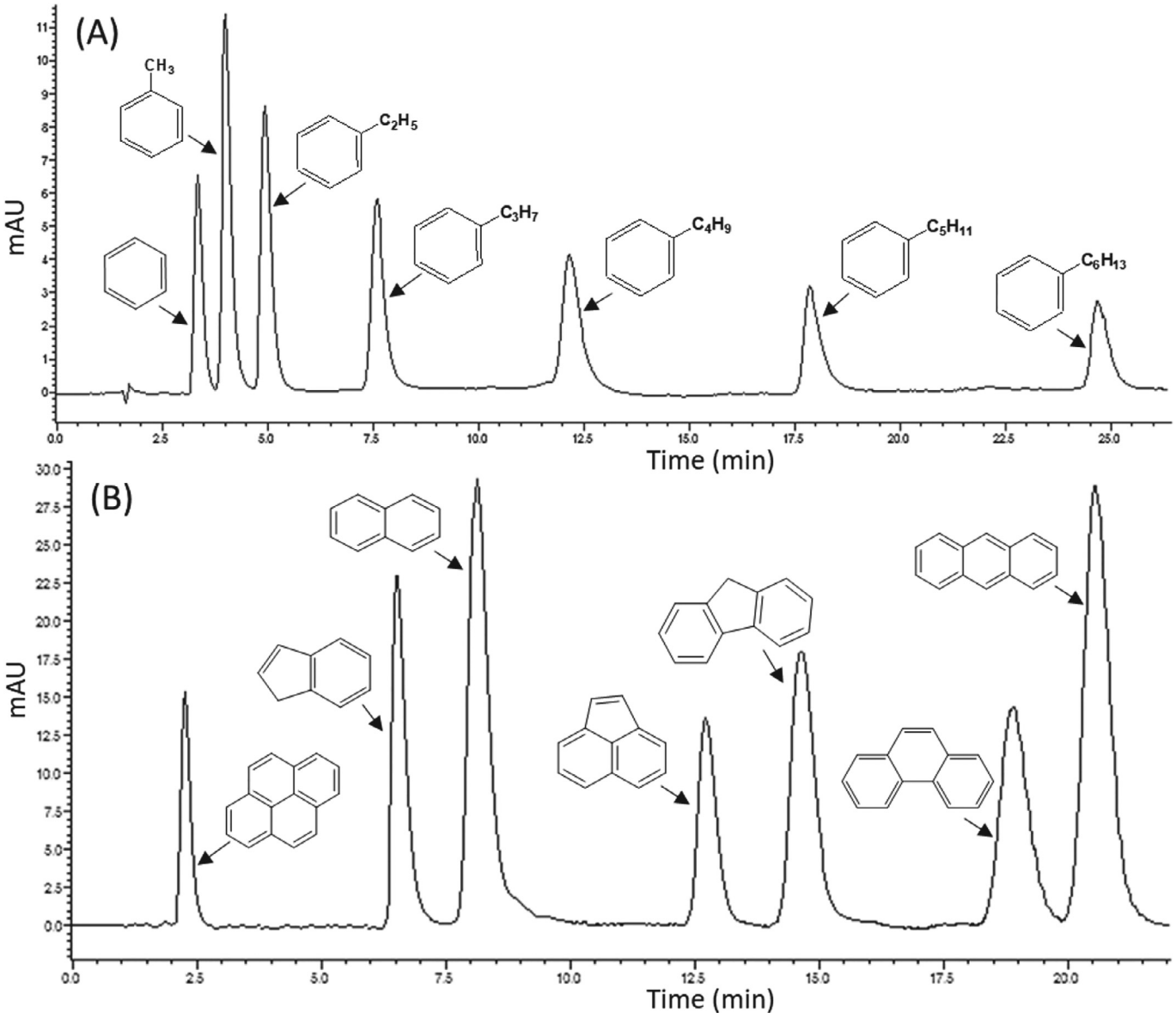


**Fig. 5.** (A) Chromatogram of the alkylbenzenes separation using MIL-53(Al) (100 mm long × 4.6 mm i.d.) column. Conditions: flow rate: 0.30 mL $min^{-1}$, detection wavelength: 254 nm, mobile phase: ACN/$H_2O$ (60:40, v/v), column temperature: 40°C. Peaks by order of elution: (1) benzene, (2) toluene, (3) *n*-ethylbenzene, (4) *n*-propylbenzene, (5) *n*-butylbenzene, (6) *n*-pentylbenzene, and (7) 1-phenylhexane. (B) Chromatogram of the separation of PAHs series using MIL-53(Al) (100 mm long × 4.6 mm i.d.) column. Conditions: flow rate: 0.35 mL $min^{-1}$, detection wavelength: 230 nm, column temperature: 30°C, mobile phase: ACN/$H_2O$ gradient elution program 0→8 min (45% ACN), 8→20 min (linear gradient 45→80% ACN), 20→22 min (80% ACN). Peaks by order of elution: (1) pyrene, (2) indene, (3) naphthalene, (4) acenaphthylene, (5) fluorene, (6) phenanthrene, and (7) anthracene.

matogram shows high-resolution baseline separation of the compounds. The elution time increases with alkyl chain length, which means that the retention time increase corresponds to the hydrophobicity of these compounds.

While the flow rate was increased from 0.10 to 0.70 mL $min^{-1}$ (Supporting Information Fig. S4), the efficiency of the column was determined in terms of the height equivalent to a theoretical plate for each compound. Fig. 3D shows the van Deemter curves for some alkylbenzenes. The prepared column exhibited the best efficiency for 1-phenylhexane with 62400 plates $m^{-1}$ at 0.30 mL $min^{-1}$. The retention times of alkylbenzenes were obviously influenced by the flow rate, whereas the change in selectivity factors was limited, not exceeding 14% between each two consecutive compounds in all experiments. As expected, with increased mobile phase flow rate, both retention and resolution decreased. However, at flow rates higher than 0.50 mL $min^{-1}$, benzene and toluene could not be separated under the isocratic mode. The chromatographic parameters of the separation of alkylbenzenes were measured at optimum conditions; they are reported in Table 1. Typically, the retention factor for the seven compounds ranged from 1.07 for benzene to 13.93 for 1-phenylhexane, while the chromatographic resolution values were higher than 2.05.

For the precision test, the injection of the alkylbenzene mixture was repeated over three successive weeks (Supporting Information Fig. S5). The RSDs of the retention time, half peak width, peak height, and peak area for three weeks on the same MIL-53(Al) column were within 0.30–0.61%, 1.43–3.10%, 1.04–2.55%, and 1.73–3.05%, respectively (Supporting Information Table S2). The obtained RSD values indicated satisfactory reproducibility.

The structure of TPA, the organic linker of MIL-53(Al), includes a benzene ring, which is assumed to provide $\pi$-$\pi$ interactions between the stationary phase and aromatic hydrocarbons [14]. For this reason, the prepared columns were used in separating a mixture of seven PAHs, which are all highly toxic for human health

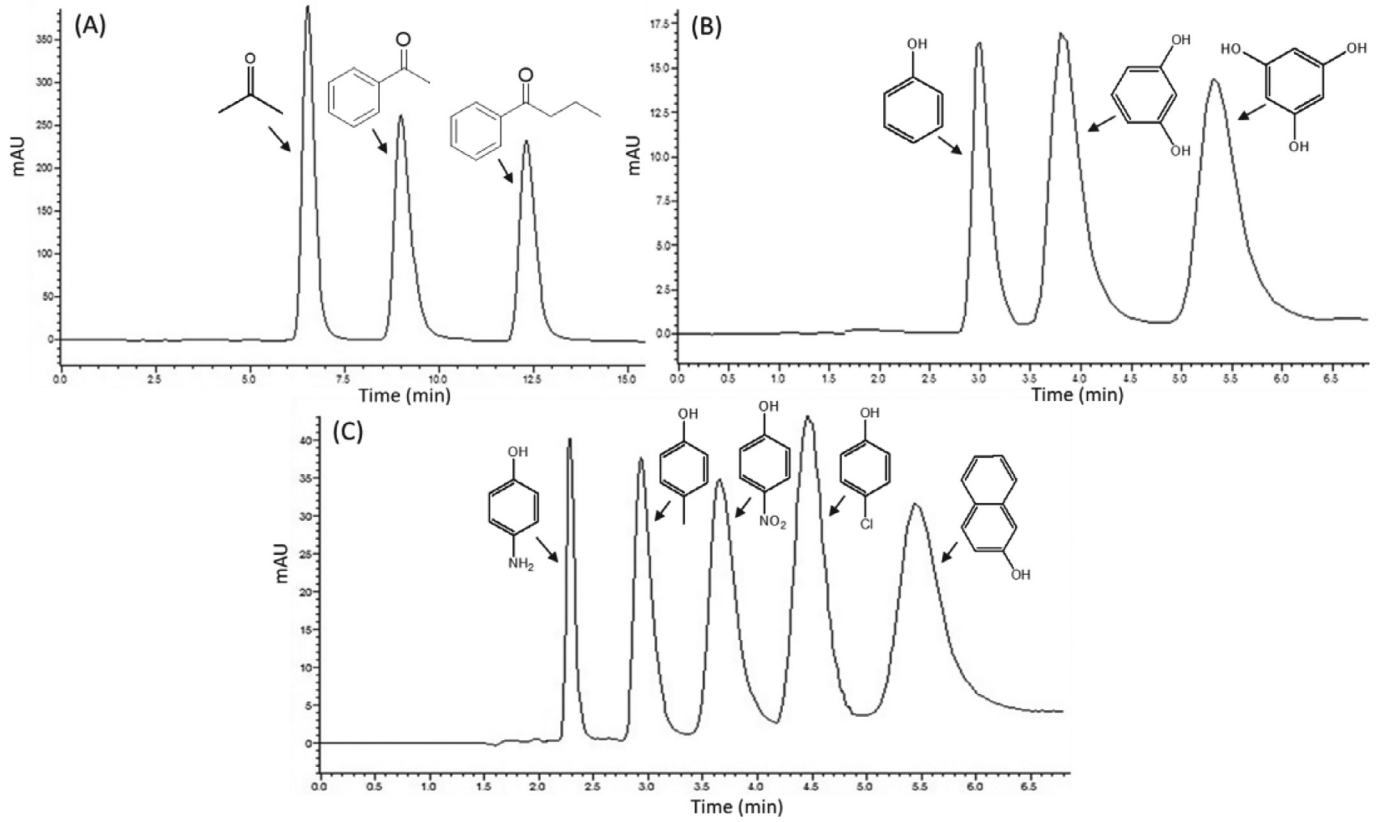


**Fig. 6.** (A) Chromatogram of the separation of ketones mixture using MIL-53(Al) (100 mm long × 4.6 mm i.d.) column. Conditions: flow rate: 0.20 mL $min^{-1}$, detection wavelength: 260 nm, mobile phase: ACN/$H_2O$ (80:20, v/v), column temperature: 40°C. Peaks by order of elution: (1) acetone, (2) acetophenone, and (3) butyrophenone. (B) Chromatogram of the separation of phenols using MIL-53(Al) (100 mm long × 4.6 mm i.d.) column. Conditions: flow rate: 0.25 mL $min^{-1}$, detection wavelength: 254 nm, mobile phase: ACN/$H_2O$ (85:15, v/v), column temperature: 30°C. Peaks by order of elution: (1) phenol, (2) resorcinol, and (3) phloroglucinol. (C) Chromatogram of the separation of some substituted phenols using MIL-53(Al) (100 mm long × 4.6 mm i.d.) column. Conditions: flow rate: 0.30 mL $min^{-1}$, detection wavelength: 254 nm, mobile phase: ACN/$H_2O$ (60:40, v/v), column temperature: 30°C. Peaks by order of elution: (1) 4-aminophenol, (2) *p*-cresol, (3) 4-nitrophenol, (4) 4-chlorophenol, and (5) 2-naphthol.

and important in environmental analysis. The effects of mobile phase composition, flow rate, and column temperature were examined to find a good compromise between peak resolution and run time. Fig. 5B represents a typical separation chromatogram for PAH compounds under optimum gradient elution conditions, using an ACN/$H_2O$ binary solvent mixture. Under validated conditions, baseline separation of the PAHs was accomplished in 22 min at a flow rate of 0.35 mL $min^{-1}$ with good chromatographic resolution. The chromatographic parameters of PAH separation were calculated at optimized conditions and are provided in Table 1. With the exception of pyrene, the height equivalent to a theoretical plate fluctuated from 0.016 to 0.070 mm for the compounds. The best efficiency was obtained for anthracene at optimal conditions, which corresponded to 63200 theoretical plates $m^{-1}$.

### 3.4.2. HPLC separation of ketonic and phenolic compounds

Subsequently, the prepared MIL-53(Al) packed column was used to separate a mixture of three ketonic compounds, acetone, acetophenone, and butyrophenone. As an example, at 0.20 mL $min^{-1}$ using the ACN/$H_2O$ (80:20, v/v) isocratic condition and a column oven temperature of 40°C, the three compounds were completely separated in 13 min with high-resolution (more than 2.81), as shown in Fig. 6A. The chromatographic parameter values were also measured and are summarized in Table 1. At the mentioned conditions, the highest performance was observed for butyrophenone with 14300 plates $m^{-1}$. On the other hand, the retention factor for the three compounds ranged between 2.92 (for acetone) to 6.47 (for butyrophenone) indicating a good balance between resolution and run time. Low peak tailing was observed for the three ketones, with asymmetry factors measured at 10% of the peak heights of 1.15, 1.26, and 1.19, respectively.

In another application, the prepared columns were used to separate two mixtures of phenolic compounds using different experimental conditions. As shown in Fig. 6B, phenol, resorcinol, and phloroglucinol were completely separated under optimal conditions, in about 6.2 min with a chromatographic resolution more than of 2.92 at a flow rate of 0.25 mL $min^{-1}$ using a mobile phase composed of ACN/$H_2O$ (85:15, v/v). The second phenolic mixture included five substituted phenols, 4-aminophenol, *p*-cresol, 4-nitrophenol, 4-chlorophenol, and 2-naphthol. They were fully separated under isocratic elution conditions at an acceptable resolution (>1.70) in 6.4 min, as presented in Fig. 6C. With the exception of 4-aminophenol, the MIL-53(Al) column did not exhibit a plate number higher than 9600 plates $m^{-1}$ at optimum conditions, where this value was notably lower than the efficiency values reached for the aromatic compounds. The retention factor values for all phenols were between 0.62 and 2.89. All of the measured chromatographic parameters are summarized in Table 1. In short, the MIL-53(Al) stationary phase clearly revealed better efficiency for the separation of neutral, non-polar, and aromatic hydrocarbons, in comparison with the slightly acidic compounds, phenols, in terms of retention, resolution, plate number, and even asymmetry factor.

### 3.4.3. HPLC separation of xylenes and methylxanthines mixtures

The columns packed with MIL-53(Al) stationary phase were also used for the separation of isomeric mixtures. Since the 100 mm long column exhibited a partial separation of xylenes and methylxanthines, the MIL-53(Al) stationary phase was packed into a 150 mm stainless-steel column to improve the chromatographic

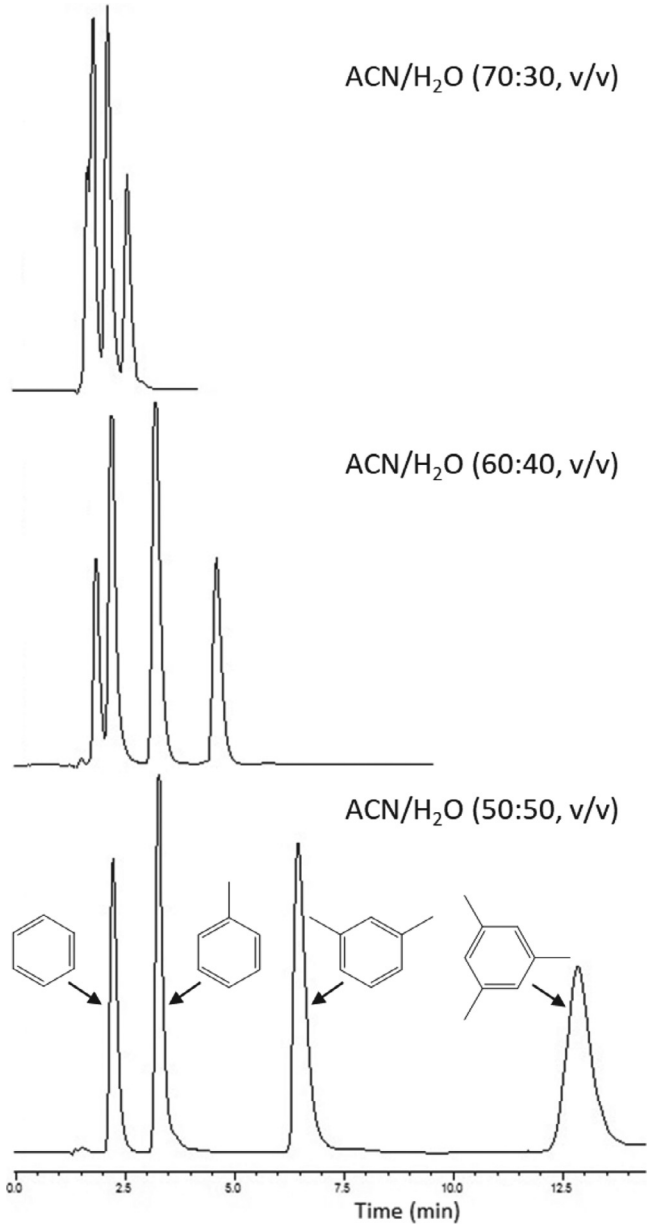


**Fig. 7.** Chromatograms for separation of some hydrocarbons on MIL-53(Al) (100 mm long × 4.6 mm i.d.) column using different ratios of the mobile phase composition (ACN/$H_2O$, v/v) at a flow rate of 0.40 mL $min^{-1}$, detection wavelength 254 nm and column oven temperature 40°C. Peaks by order of elution: (1) benzene, (2) toluene, (3) *m*-xylene, and (4) mesitylene.

resolution. In spite of this, no significant increase in column backpressure was observed due to the high structural porosity of the MOFs material. An excellent baseline separation of *o*-, *m*-, and *p*-xylenes mixture (Fig. 4A) was achieved using this prepared column in approximately 11 min, with an ACN/$H_2O$ (65:35, v/v) mixture as the mobile phase at 0.35 mL $min^{-1}$ flow rate. Of the three xylenes, the ortho-isomer showed the highest affinity to the structure of MIL-53(Al) due to its polarity and the interaction between the two ortho-$CH_3$ groups and the terephthalate pore walls of the MIL-53(Al) stationary phase [32].

High-resolution separation was also accomplished for the other mixture including theobromine, theophylline, and caffeine, as shown in Fig. 4B. The analytes were separated using a binary ACN/$H_2O$ (70:30, v/v) composition at a flow rate of 0.25 mL $min^{-1}$ in 18 min. The solutes were detected at 273 nm UV wavelength. These results confirmed the remarkable ability of the MIL-53(Al) stationary phase for the discrimination of structural isomers. Among the xylenes, the best efficiency was 7000 plates $m^{-1}$ for *p*-xylene, while for xanthines, the plate number for theobromine was 30200 plates $m^{-1}$ at optimum conditions. The highest retention factors were 2.39 and 4.06 for *o*-xylene and caffeine, respectively, while the chromatographic resolution between the peaks was more than 2.59 in all cases. All of the separation parameters for the two mixtures are provided in Table 1.

**Table 1**
Peak parameters for the separation of alkylbenzene, PAH, ketonic, and phenolic mixtures with MIL-53(Al) 100 mm long column and xylene and xanthine mixtures with MIL-53(Al) 150 mm long column under the optimized conditions for each mixture

| analyte | $t_R$ | N | k | $\alpha$ | $R_s$ | $A_s$ |
|---|---|---|---|---|---|---|
| benzene | 3.42 | 10700 | 1.07 | – | – | 1.23 |
| toluene | 4.24 | 12400 | 1.57 | 1.66 | 2.05 | 1.25 |
| ethylbenzene | 5.09 | 13900 | 2.08 | 1.53 | 2.25 | 1.16 |
| n-propylbenzene | 7.61 | 20400 | 3.61 | 1.93 | 5.13 | 1.08 |
| n-butylbenzene | 12.35 | 34300 | 6.48 | 2.01 | 7.77 | 1.31 |
| n-pentylbenzene | 17.86 | 62100 | 9.82 | 1.71 | 7.83 | 1.17 |
| 1-phenylhexane | 24.63 | 62400 | 13.93 | 1.62 | 7.89 | 1.28 |
| pyrene | 2.27 | 5700 | 0.37 | – | – | 1.21 |
| indene | 6.58 | 19900 | 2.99 | 7.95 | 11.05 | 1.28 |
| naphthalene | 8.17 | 14300 | 3.95 | 1.32 | 2.72 | 1.32 |
| acenaphthylene | 12.73 | 20800 | 6.72 | 1.70 | 5.72 | 1.20 |
| fluorene | 14.62 | 23700 | 7.86 | 1.17 | 2.04 | 1.22 |
| phenanthrene | 18.91 | 60800 | 10.46 | 1.33 | 4.91 | 1.34 |
| anthracene | 20.54 | 63200 | 11.45 | 1.09 | 2.02 | 1.33 |
| acetone | 6.47 | 6100 | 2.92 | – | – | 1.15 |
| acetophenone | 8.92 | 10300 | 4.41 | 1.71 | 2.81 | 1.26 |
| butyrophenone | 12.33 | 14300 | 6.47 | 1.67 | 3.50 | 1.19 |
| phenol | 2.97 | 12400 | 1.12 | – | – | 1.36 |
| resorcinol | 3.81 | 9000 | 1.72 | 1.74 | 2.48 | 1.42 |
| phloroglucinol | 5.33 | 7900 | 2.81 | 1.83 | 2.99 | 1.48 |
| 4-aminophenol | 2.27 | 22900 | 0.62 | – | – | 1.24 |
| p-cresol | 2.94 | 9600 | 1.10 | 1.97 | 2.93 | 1.33 |
| 4-nitrophenol | 3.62 | 8200 | 1.59 | 1.64 | 1.91 | 1.45 |
| 4-chlorophenol | 4.47 | 7900 | 2.19 | 1.58 | 1.86 | 1.38 |
| 2-naphthol | 5.45 | 7400 | 2.89 | 1.52 | 1.70 | 1.48 |
| p-xylene | 5.14 | 7000 | 0.83 | – | – | 1.27 |
| m-xylene | 6.72 | 6100 | 1.40 | 1.86 | 2.59 | 1.36 |
| o-xylene | 9.53 | 5600 | 2.39 | 1.99 | 3.16 | 1.43 |
| theobromine | 8.51 | 30200 | 1.57 | – | – | 1.22 |
| theophylline | 10.46 | 15600 | 2.16 | 1.57 | 3.54 | 1.23 |
| caffeine | 16.72 | 15500 | 4.06 | 2.06 | 6.90 | 1.30 |

$t_R$: retention time (min), *N*: number of theoretical plates ($m^{-1}$), *k*: retention factor, $\alpha$: selectivity factor, $R_s$: chromatographic resolution, and $A_s$: asymmetry factor at 10% of peak heights.

The reproducibility of separation results obtained for xylenes and methylxanthines was expressed in terms of %RSD for three weeks on the same column. The column showed a good reproducibility with RSD values ≤0.57% for retention time, ≤3.77% for half peak width, ≤3.05% for peak height, and ≤3.88% for peak area in all cases (Supporting Information Table S2 and Figs. S6 & S7).

To complete the picture, the applicability of the prepared MIL-53(Al) packed columns for analysis of real samples was demonstrated by injecting a green tea water extract. Tea extract is a typical mixture used to examine column performance because it normally consists of many organic compounds related to various chemical species such as phenolic acids, catechins, and methylxanthines. Fig. 4C shows the successful separation of a green tea water extract components. Under optimal conditions, a satisfactory separation was obtained for the tea sample constituents with reasonable resolution ($R_s \geq 0.94$). In contrast to $C_{18}$ columns, catechins such as (+)-catechin, (-)-epicatechin, or (-)-epigallocatechin were eluted on MIL-53(Al) before the three methylxanthines regardless of the mobile phase composition as a result of size-exclusion. On the other hand, the retention order of gallic acid, theobromine, theophylline, and caffeine remained in accordance with their hy-

**Table 2**
Values of $\Delta H$, $\Delta S$, $\Delta G$ (at different temperatures from 30–50°C), and $R^2$ for xylenes and methylxanthines

| analyte | $\Delta H$ | $\Delta S$ | $\Delta G$ | | | | | $R^2$ |
|---|---|---|---|---|---|---|---|---|
| | | | 30°C | 35°C | 40°C | 45°C | 50°C | |
| *p*-xylene | -11.35 | -32.74 | -1.43 | -1.27 | -1.10 | -0.94 | -0.78 | 0.9886 |
| *m*-xylene | -10.28 | -26.21 | -2.34 | -2.21 | -2.08 | -1.94 | -1.81 | 0.9890 |
| *o*-xylene | -10.39 | -14.35 | -6.04 | -5.97 | -5.90 | -5.83 | -5.75 | 0.9822 |
| theobromine | -10.06 | -25.61 | -2.30 | -2.17 | -2.04 | -1.92 | -1.79 | 0.9935 |
| theophylline | -10.59 | -22.15 | -3.88 | -3.77 | -3.66 | -3.55 | -3.44 | 0.9981 |
| caffeine | -9.75 | -12.53 | -5.96 | -5.89 | -5.83 | -5.77 | -5.71 | 0.9948 |

$\Delta H$ (kJ mol$^{-1}$), $\Delta S$ (J mol$^{-1}$ K$^{-1}$), and $\Delta G$ (kJ mol$^{-1}$).

drophobicity. In conclusion, the ability of the MIL-53(Al) column to separate complex samples with adequate resolution and efficiency gives it an additional advantage.

### 3.5. Effect of analyte mass

The effect of the injected analyte mass on the prepared columns was also studied. As shown in Fig. 8A for xylene isomers and Fig. S8A (Supporting Information) for methylxanthines, an increase in the analyte mass resulted in increased peak height and area, while the retention time was almost unchanged. The relationship between analyte mass and chromatographic peak height and area was linear over the investigated mass ranges (Fig. 8B and Supporting Information Fig. S8B). Practically, the selectivity factors remained constant at values of 1.89/1.99 (±0.02) for xylenes and 1.58/2.05 (±0.01) for methylxanthines (Supporting Information Tables S3 & S4). These features illustrate the MIL-53(Al) suitability for full separation and accurate quantitation of xylenes and methylxanthines.

### 3.6. Effect of temperature and thermodynamic parameters measurement

To obtain more information about the retention of the analytes on the MIL-53(Al) columns, xylenes and methylxanthines mixtures were injected at temperatures from 30 to 50°C. The retention time of the analytes gradually decreased as the column temperature increased, as exhibited in Fig. 9A and Fig. S9A (Supporting Information), indicating an exothermic separation process of the analytes on the MIL-53(Al) stationary phase. The selectivity factors for *p*- and *m*-xylenes, theobromine, and theophylline slightly decreased, while the selectivity values for *o*-xylene and caffeine even slightly increased as the temperature increased (Supporting Information Tables S5 & S6). However, the results verify the high selectivity of MIL-53(Al) toward *o*-xylene and caffeine.

The van't Hoff plots for the separation of xylenes (Fig. 9B) and methylxanthines (Supporting Information Fig. S9B) have been used to demonstrate the relationship between retention factor and column temperature. Good linearity between ln $k$ and 1/T was deemed due to regression factors ≥0.9822, suggesting that there was no change in the interaction mechanism for the studied solutes in the temperature range between 30 and 50°C. The thermodynamic parameters $\Delta H$, $\Delta S$, and $\Delta G$ (at different temperature) for the transfer of xylene and methylxanthine analytes from the mobile phase to the stationary phase of MIL-53(Al) are presented in Table 2. For all analytes, the values of $\Delta H$ were negative while the $\Delta S$ had small negative values; this corresponds to a favorable transfer of the analytes from the mobile phase to the stationary phase, and thus stronger retention for the solutes on the MIL-53(Al). The weak negative values of $\Delta S$ along with the comparable values of $\Delta H$ for xylene isomers, as well as for methylxanthines, suggested that the highly selective retention of *o*-xylene and caffeine on MIL-53(Al) was not based on $\Delta H$, but controlled by $\Delta S$. On the other hand, the negative values of $\Delta G$ reveal that the transfer of xylene and methylxanthine analytes from the mobile phase to the MIL-53(Al) was with a thermodynamically spontaneous process. Again, the retention of *o*-xylene and caffeine on MIL-53(Al) corresponded to more negative $\Delta G$ values in comparison with the two other compounds in the same mixture, thus resulting in stronger retention for those solutes on the MIL-53(Al) stationary phase. It could be also noted that the values of $\Delta G$ gradually decreased as the column temperature increased, thus stronger retention for all solutes on MIL-53(Al) occurred at lower temperatures.

### 3.7. Comparison with other works

A series of synthesized MOFs were investigated as the stationary phase in its naked structure for packed HPLC columns [32,33,43–63]. Table 3 provides a summary of several MOF materials used for HPLC separation, listing the analytes, column dimensions, mobile phase solvents, and some important separation parameters. In particular, the MIL-*n* class of MOFs attracted wide attention due to its good chemical and water stability in addition to their attractive properties such as large surface area; these make them promising stationary phases for HPLC separation and analysis of various compounds. Many interesting applications including environmental and industrial chemicals were successfully developed by using various MOFs. Most of these applications were carried out under NP non-aqueous mobile phases or even by using a pure solvent as mobile phase.

With the exception of MIL-101(Cr) that had been post-synthetically modified with pyridine, all naked MOFs used as stationary phase did not exhibit column efficiencies higher than 23700 plates m$^{-1}$ for the same analyte categories. The literature survey indicated that the green method used for synthesis of MIL-53(Al) from PET waste water bottles in this work is completely original for chromatographic applications. Compared with previously cited MOFs packed columns, the present MIL-53(Al) columns gave comparable selectivity and much better efficiency for most of the studied chemicals at optimum conditions, indicating the feasibility of MIL-53(Al) as a stationary phase for HPLC applications. The prepared MIL-53(Al) column was compared with the most widely used conventional particulate octadecyl-silica column packed with 5 $\mu$m and possessing the same dimensions as the prepared column (150 mm long × 4.6 mm i.d.). Each column was run at its optimum conditions to compromise between chromatographic resolution and the run time for the separation of theobromine, theophylline, and caffeine. The results and discussion of this part are demonstrated in the Supporting Information.

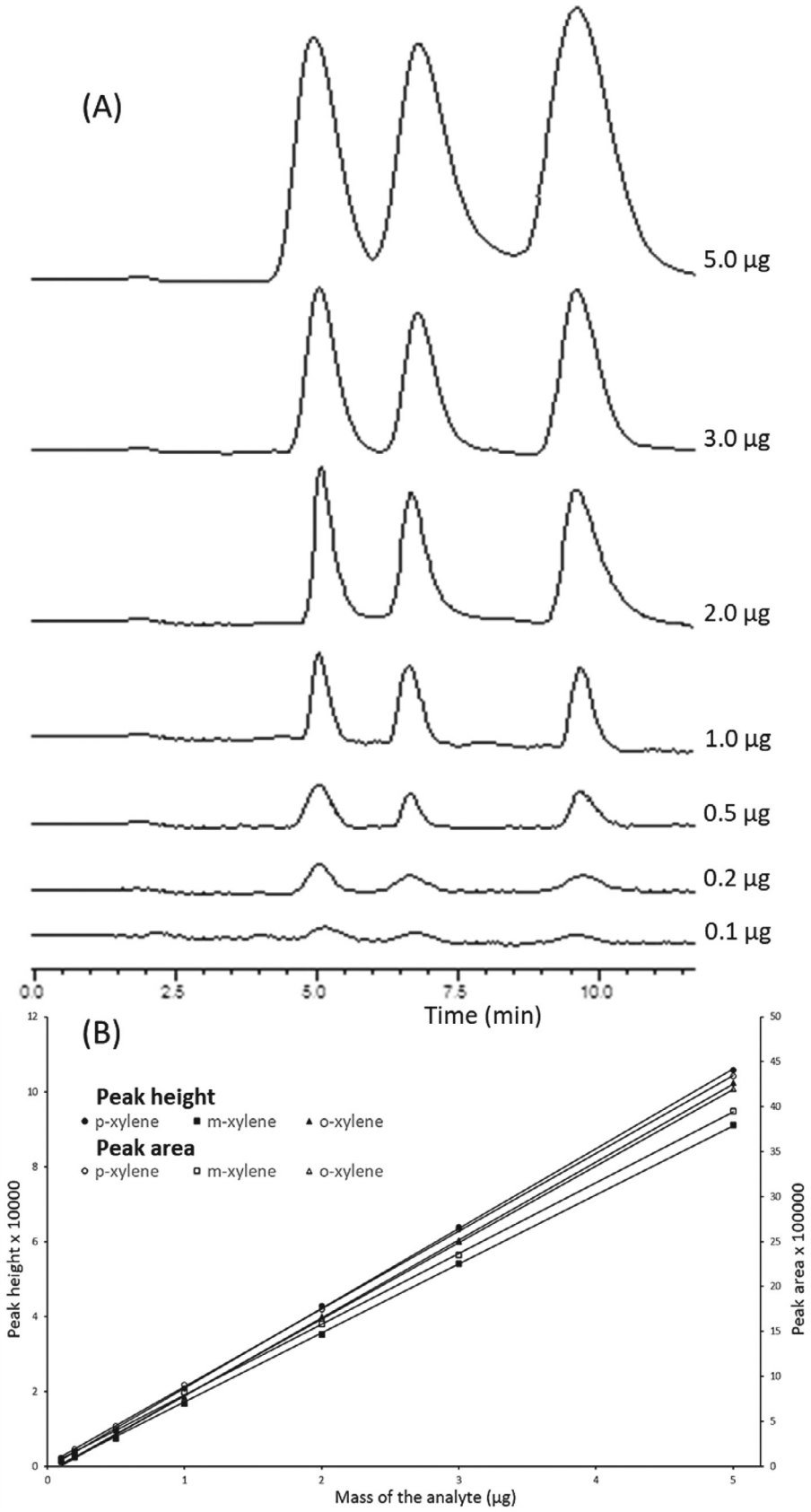


**Fig. 8.** (A) Chromatograms of xylene isomers with different injected masses. (B) Effect of the injected mass of xylene isomers on the peaks area and height using MIL-53(Al) (150 mm long × 4.6 mm i.d.) column. Separation conditions are as shown in Fig. 7A.

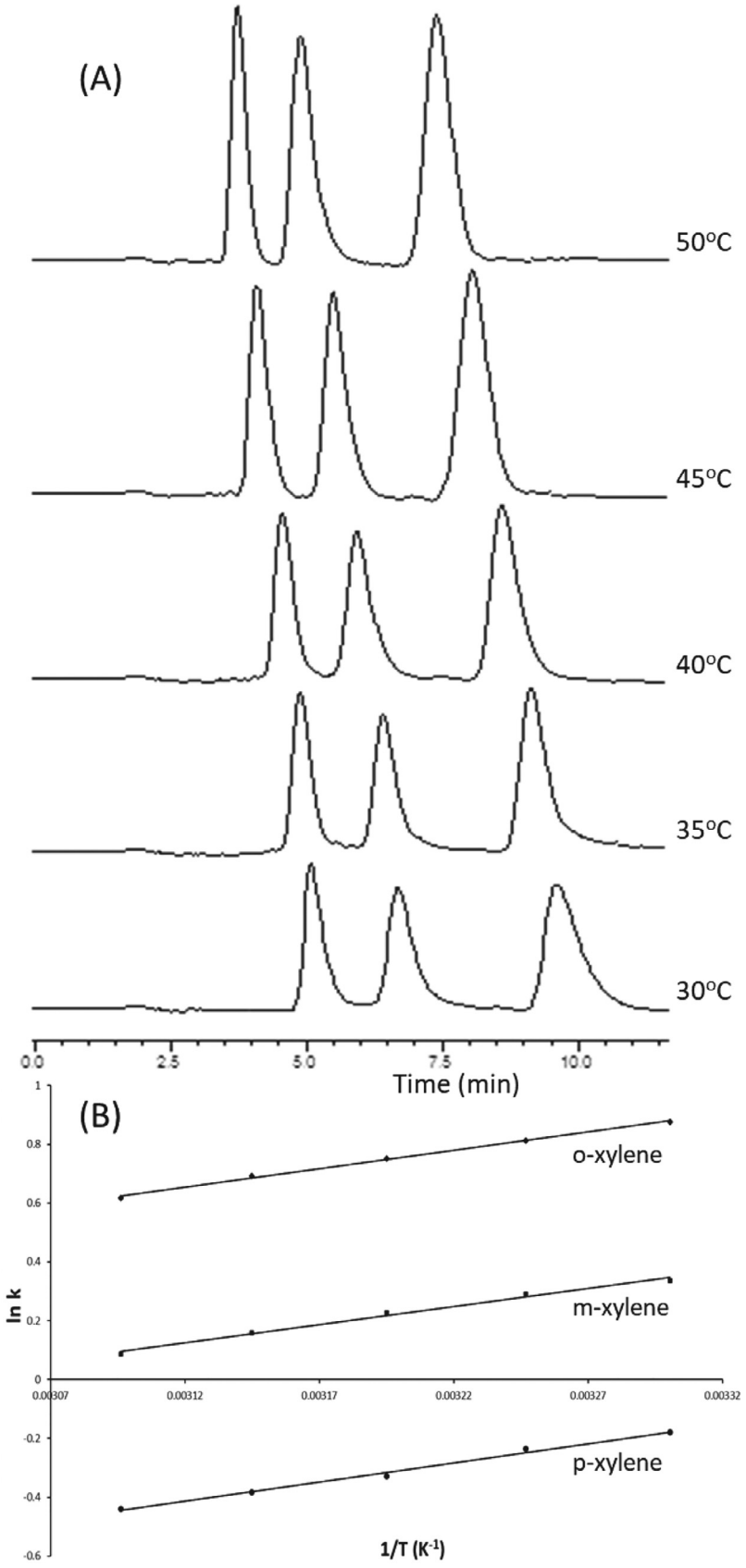


**Fig. 9.** (A) Chromatograms of xylene isomers at different column temperatures (30–50°C). (B) van't Hoff plots xylene isomers on the MIL-53(Al) packed column (150 mm long × 4.6 mm i.d.). Separation conditions are as shown in Fig. 7A.

**Table 3**
Applications of different MOF materials as stationary phases for HPLC separation

| MOF | analytes | solvents | $\alpha$ | $N_{max}$ | column description (mm long × mm i.d.) | ref. |
|---|---|---|---|---|---|---|
| MIL-53(Al) | alkylbenzenes, PAHs, ketones, phenols, xylene isomers, and methylxanthines | ACN/$H_2O$ | 1.09–7.95 | 63200 for anthracene | 100, & 150 × 4.6 | This work |
| MIL-101(Cr) | xylene, dichlorobenzenes, and chlorotoluene isomers, ethylbenzene, styrene, and toluene | hexane/DCM | 1.16–2.36 | 20000 for ethylbenzene | 50 × 4.6 | [32] |
| MIL-53(Fe) | xylene, dichlorobenzene, chlorotoluene, and nitroaniline isomers, alkylbenzenes, anilines, and PAHs | ACN/$H_2O$ | 0.82–2.33 | 3272 for o-nitroaniline | 200 × 2.1 | [33] |
| MIL-53(Al) | toluene and ethylbenzene, PAHs, benzenediol isomers, anilines, and xanthines | ACN/$H_2O$ | – | 23705 for bromobenzene | 70 × 4.6 | [43] |
| MIL-53(Al) | xylenes and ethylbenzene, ethyltoluenes, and cymenes | hexane | 0.5–10.9 | – | 50 × 4.0 | [44] |
| MIL-47 | xylene isomers and ethylbenzene | hexane | 0.10–10.9 | – | 50 × 4.0 | [45] |
| MIL-100(Fe) | aromatic hydrocarbons and anilines, toluidine and chloroaniline isomers | DCM/MeOH, MeOH/$H_2O$ | 1.33–3.25 | 11262 for o-chloroaniline | 50 × 4.6 | [46] |
| MIL-53(Al) | phthalate acid esters | MeOH/$H_2O$ | 1.33–2.63 | – | 50 × 4.6 | [47] |
| MIL-125(Ti) | xylene and methylacetophenone isomers, PAHs, aryl halides, alkyl and hetero aromatics, and cis/trans cyclohexane | ACN | 1.01–6.66 | 20000 for benzene | 100 × 2.1 | [48] |
| MIL-100(Fe) | aromatic hydrocarbons; toluene, styrene, *p*-xylene, acetanilide, 2-nirtoaniline, and 1-naphthylamine | MeOH/$H_2O$ | – | – | 200 × 1.0 | [49] |
| UiO-66 | PAHs, substituted benzenes and its isomers | hexane/DCM, MeOH/$H_2O$ | 1.38–1.85 | 2154 for *m*-xylene | 50 × 4.6 | [50] |
| DUT-67(Zr) | xylene isomers and phthalate acid esters | MeOH/$H_2O$ | 1.20–2.00 | – | 50 × 4.6 | [51] |
| MIL-101(Cr) | nitroaniline, aminophenol, and naphthol isomers, sulfadimidine and sulfanilamide | DCM/MeOH | – | – | 50 × 4.6 | [52] |
| MIL-101(Cr) | fullerenes $C_{60}$, $C_{70}$, and high fullerenes | DCM/ACN | 17.1 | 13000 for $C_{70}$ | 50 × 4.6 | [53] |
| HKUST-1 | ethylbenzene and styrene | heptane/DCM | – | – | 50 × 4.6 | [54] |
| HKUST-1, MOF-5 | aromatic hydrocarbons | hexane/DCM | – | – | 150 & 250 × 4.6 | [55] |
| ZIF-8, HKUST-1, Basolite F300, MIL-47 | small intermediates and byproducts found in the active pharmaceuticals | MeOH | 1.16–180 | 1640 for 3-(1-hydroxyphenyl) ethanol | 50 × 4.6 | [56] |
| MIL-47, MIL-53(Al) | ethylbenzene and styrene | heptane | 3.6, 4.1 | – | 50 × 4.5 | [57] |
| MIL-53(Fe) | BTEX compounds | heptane | 1.0–12.26 | – | 50 × 4.6 | [58] |
| MIL-53(Al) | xylene, dichlorobenzene, chlorotoluene, and nitrophenol isomers | hexane/DCM, DCM/MeOH | 1.13–3.29 | 10200 for ethylbenzene | 150 × 4.6 | [59] |
| UiO-66 | benzene, benzyl alcohol, phenol, chlorobenzene, benzyl chloride, and cis/trans 4-ethylcyclohexanol, | MeOH/ACN | 0.40–6.9 | – | 50 × 4.6 | [60] |
| MIL-125(Ti), MIL-125(Ti)-$NH_2$, CAU-1(Al)-$NH_2$ | xylene, ethyltoluene, and cymene isomers | heptane | 3.1 | – | 50 × 4.5 | [61] |
| MIL-101(Cr)-pyridine | tocopherols | hexane/IPA | – | 85000 for $\delta$-tocopherol | 50 × 4.6 | [62] |
| MIL-125(Ti) | ethylbenzene and xylene isomers | heptane | 0.7–1.6 | – | 100 × 4.6 | [63] |

$N_{max}$: maximum number of theoretical plates ($m^{-1}$).

## 4. Conclusions

In our green approach, waste PET bottle materials were successfully used as the starting precursor instead of TPA for the synthesis of MIL-53(Al) MOF. The slurry packed MIL-53(Al) HPLC columns were explored for separation of a wide range of analytes including alkylbenzenes, PAHs, ketones, phenols, and isomeric compounds, in addition to green tea water extract using different compositions of a binary ACN/$H_2O$ mobile phase in isocratic and gradient modes. For all studied analytes, the optimum conditions and evaluation parameters for separation and qualitative analysis were investigated in detail. The prepared columns showed better separation of alkylbenzenes and PAHs in terms of separation efficiency and peak shape. Among the classical MOFs used as stationary phases in HPLC, the present research exhibited MIL-53(Al) packed columns with much better efficiency and resolution for most of the studied chemicals at optimum conditions. The results obtained using waste PET bottles confirmed the effectiveness of MOF preparation and its applications. In comparison with previously published MOFs packed columns in terms of chromatographic parameters and separation performance, the present MIL-53(Al) columns gave comparable selectivity and better efficiency for most of the studied mixtures at optimum conditions. The present work points out continued interest in using value-added materials from waste for synthesis and application of many important MOFs materials with more environmental and economic benefits.

## Authorship contributions

**Category 1**

-Conception and design of study:

Ahmad Aqel, Zeid A. ALOthman, Ahmed-Yacine Badjah-Hadj-Ahmed

-Acquisition of data:

Ahmad Aqel, Norah Alkatheri, Ayman A. Ghfar, Ameen M. Al-subhi

-Analysis and/or interpretation of data:

Ahmad Aqel, Zeid A. ALOthman, Ahmed-Yacine Badjah-Hadj-Ahmed

**Category 2**

-Drafting the manuscript:

Ahmad Aqel, Ahmed-Yacine Badjah-Hadj-Ahmed

-Revising the manuscript critically for important intellectual content:

Norah Alkatheri, Ayman A. Ghfaar, Ameen M. Alsubhi, Zeid A. ALOthman

**Category 3**

-Approval of the version of the manuscript to be published:

Ahmad Aqel, Norah Alkatheri, Ayman A. Ghfar, Ameen M. Alsubhi, Zeid A. ALOthman, Ahmed-Yacine Badjah-Hadj-Ahmed

## Declaration of Competing Interest

The authors declare that they have no known competing financial interests or personal relationships that could have appeared to influence the work reported in this paper.

## Acknowledgment

The authors extend their appreciation to the Deanship of Scientific Research at King Saud University for funding this work through research group No (RG-1437-011). The authors thank the Deanship of Scientific Research and RSSU at King Saud University for their technical support.

## Supplementary materials

Supplementary material associated with this article can be found, in the online version, at doi:10.1016/j.chroma.2020.461857.

## References

[1] H. Li, M. Eddaoudi, M. O'Keeffe, O.M. Yaghi, Design and synthesis of an exceptionally stable and highly porous metal-organic framework, Nature 402 (1999) 276–279.
[2] H. Furukawa, K.E. Cordova, M. O'Keeffe, O.M. Yaghi, The chemistry and applications of metal-organic frameworks, Science 341 (2013) 1230444, doi:10.1126/science.1230444.
[3] L.J. Murray, M. Dinca, J.R. Long, Hydrogen storage in metal–organic frameworks, Chem. Soc. Rev. 38 (2009) 1294–1314, doi:10.1039/B802256A.
[4] J.-R. Li, J. Sculley, H.-C. Zhou, Metal–organic frameworks for separations, Chem. Rev. 112 (2012) 869–932, doi:10.1021/cr200190s.
[5] M.S. El-Shall, V. Abdelsayed, A.E.S. Khder, H.M.A. Hassan, H.M. El-Kaderi, T.E. Reich, Metallic and bimetallic nanocatalysts incorporated into highly porous coordination polymer MIL-101, J. Mater. Chem. 19 (2009) 7625–7631, doi:10.1039/B912012B.
[6] N. Manousi, G.A. Zachariadis, E.A. Deliyanni, V.F. Samanidou, Applications of metal-organic frameworks in food sample preparation, Molecules 23 (2018) 2896–2917, doi:10.3390/molecules23112896.
[7] L.E. Kreno, K. Leong, O.K. Farha, M. Allendorf, R.P. Van Duyne, J.T. Hupp, Metal-organic framework materials as chemical sensors, Chem. Rev. 112 (2012) 1105–1125, doi:10.1021/cr200324t.
[8] J. Yang, Y.-W. Yang, Metal–organic frameworks for biomedical applications, Small 16 (2020) 1906846, doi:10.1002/smll.201906846.
[9] P. Horcajada, C. Serre, M. Vallet-Regi, M. Sebban, F. Taulelle, G. Férey, Metal-Organic Frameworks as Efficient Materials for Drug Delivery, Angew. Chem. Int. Ed. 45 (2006) 5974–5978, doi:10.1002/anie.200601878.
[10] P.-L. Wang, L.-H. Xie, E.A. Joseph, J.-R. Li, X.-O. Su, H.-C. Zhou, Metal-organic frameworks for food safety, Chem. Rev. 119 (2019) 10638–10690, doi:10.1021/acs.chemrev.9b00257.
[11] K.M.L. Taylor-Pashow, J. Della Rocca, Z.G. Xie, S. Tran, W.B. Lin, Postsynthetic modifications of iron-carboxylate nanoscale metal–organic frameworks for imaging and drug delivery, J. Am. Chem. Soc. 131 (2009) 14261–14263, doi:10.1021/ja906198y.
[12] H. Kim, S. Yang, S.R. Rao, S. Narayanan, E.A. Kapustin, H. Furukawa, A.S. Umans, O.M. Yaghi, E.N. Wang, Water harvesting from air with metal-organic frameworks powered by natural sunlight, Science 356 (2017) 430–434, doi:10.1126/science.aam8743.
[13] T. Qiu, Z. Liang, W. Guo, H. Tabassum, S. Gao, R. Zou, Metal–organic framework-based materials for energy conversion and storage, ACS Energy Lett 5 (2020) 520–532, doi:10.1021/acsenergylett.9b02625.
[14] Y. Yu, Y. Ren, W. Shen, H. Deng, Z. Gao, Applications of metal-organic frameworks as stationary phases in chromatography, TrAC Trends in Analytical Chemistry 50 (2013) 33–41, doi:10.1016/j.trac.2013.04.014.
[15] J. Zhang, Z. Chen, J. Chromatogr. A Metal-organic frameworks as stationary phase for application in chromatographic separation, 1530 (2017) 1–18. https://doi.org/10.1016/j.chroma.2017.10.065.
[16] K. Yusuf, A. Aqel, Z. ALOthman, Metal-organic frameworks in chromatography, J. Chromatogr. A 1348 (2014) 1–16, doi:10.1016/j.chroma.2014.04.095.
[17] Z.-Y. Gu, C.-X. Yang, N. Chang, X.-P. Yan, Metal–organic frameworks for analytical chemistry: From sample collection to chromatographic separation, Acc. Chem. Res. 45 (2012) 734–745, doi:10.1021/ar2002599.
[18] X. Zhao, Y. Wang, D.-S. Li, X. Bu, P. Feng, Metal-organic frameworks for separation, Adv. Mater. 30 (2018) 1705189, doi:10.1002/adma.201705189.
[19] X. Wang, N. Ye, Recent advances in metal-organic frameworks and covalent organic frameworks for sample preparation and chromatographic analysis, Electrophoresis 38 (2017) 3059–3078, doi:10.1002/elps.201700248.
[20] Q. Wei, C. Lian, H. Su, D. Gao, S. Wang, Composite of ZIF-8 and totally porous silica gel for HPLC stationary phase, Micropor. Mesopor. Mat. 288 (2019) 109574–109579, doi:10.1016/j.micromeso.2019.109574.
[21] K. Yusuf, A.-Y. Badjah-Hadj-Ahmed, A. Aqel, T. Aouak, Z.A. ALOthman, Zeolitic imidazolate framework-methacrylate composite monolith characterization by inverse gas chromatography, J. Chromatogr. A 1443 (2016) 233–240, doi:10.1016/j.chroma.2016.03.025.
[22] X. Yang, C. Li, M. Qi, L. Qu, Graphene-ZIF8 composite material as stationary phase for high-resolution gas chromatographic separations of aliphatic and aromatic isomers, J. Chromatogr. A 1460 (2016) 173–180, doi:10.1016/j.chroma.2016.07.029.
[23] R.I. Walton, Subcritical solvothermal synthesis of condensed inorganic materials, Chem. Soc. Rev. 31 (2002) 230–238, doi:10.1039/B105762F.
[24] F. Millange, C. Serre, G. Férey, Synthesis, structure determination and properties of MIL-53as and MIL-53ht: the first Criii hybrid inorganic–organic microporous solids: $Cr^{III}(OH)\bullet\{O_2C–C_6H_4–CO_2\}\bullet\{HO_2C–C_6H_4–CO_2H\}_x$, Chem. Commun (2002) 822–823, doi:10.1039/B201381A.
[25] T. Loiseau, C. Serre, C. Huguenard, G. Fink, F. Taulelle, M. Henry, T. Bataille, G. Férey, A rationale for the large breathing of the porous aluminum terephthalate (MIL-53) upon hydration, Chem. Eur. J. 10 (2004) 1373–1382, doi:10.1002/chem.200305413.
[26] S.B. Wang, C.S. Wang, H.P. Wang, X.L. Chen, S.B. Wang, Sodium titanium tris(glycolate) as a catalyst for the chemical recycling of poly(ethylene terephthalate) via glycolysis and repolycondensation, Polym. Degrad. Stab. 114 (2015) 105–114, doi:10.1016/j.polymdegradstab.2015.02.006.
[27] F. Awaja, S. Pavel, Recycling of PET, Eur. Polym. J. 41 (2005) 1453–1477, doi:10.1016/j.eurpolymj.2005.02.005.
[28] X. Dyosiba, J. Ren, N.M. Musyoka, H.W. Langmi, M. Mathe, M.S. Onyango, Preparation of value-added metal-organic frameworks (MOFs) using waste PET bottles as source of acid linker, SM&T 10 (2016) 10–13, doi:10.1016/j.susmat.2016.10.001.
[29] S. Cavalcante, D. Vieira, I. Melo, Chemical recycling: Comparative study about the depolymerization of PET waste-bottles to obtain terephthalic acid, Proceedings 41 (2019) 78–86, doi:10.3390/ecsoc-23-06650.
[30] J. Ren, X. Dyosiba, N.M. Musyoka, H.W. Langmi, B.C. North, M. Mathe, M.S. Onyango, Green synthesis of chromium-based metal-organic framework (Cr-MOF) from waste polyethylene terephthalate (PET) bottles for hydrogen storage applications, Int. J. Hydrog. Energy 41 (2016) 18141–18146, doi:10.1016/j.ijhydene.2016.08.040.
[31] S.-H. Lo, D.S. Raja, C.-W. Chen, Y.-H. Kang, J.-J. Chen, C.-H. Lin, Waste polyethylene terephthalate (PET) materials as sustainable precursors for the synthesis of nanoporous MOFs, MIL-47, MIL-53(Cr, Al, Ga) and MIL-101(Cr), Dalton Trans 45 (2016) 9565–9573, doi:10.1039/C6DT01282E.
[32] C.-X. Yang, X-P. Yan, Metal-organic framework MIL-101(Cr) for high-performance liquid chromatographic separation of substituted aromatics, Anal. Chem. 83 (2011) 7144–7150, doi:10.1021/ac201517c.
[33] Z. Yan, W. Zhang, J. Gao, Y. Lin, J. Li, Z. Lin, L. Zhang, Reverse-phase high performance liquid chromatography separation of positional isomers on a MIL-53(Fe) packed column, RSC Adv 5 (2015) 40094–40102, doi:10.1039/C5RA02262B.
[34] L. Reich, S.S. Stivala, in: Elements of polymer degradation, McGraw Hill, New York, 1971, p. 361.
[35] R.J. Ehrig, in: Plastics recycling: products and processes, Hanser Publishers, New York, 1992, p. 1992.
[36] L.F. Gomez, R. Zacharia, P. Bénard, R. Chahine, Simulation of binary $CO_2/CH_4$ mixture breakthrough profiles in MIL-53 (Al), J. Nanomaterials 2015 (2015) 439382, doi:10.1155/2015/439382.
[37] C. Li, Z. Xiong, J. Zhang, C. Wu, The strengthening role of the amino group in metal–organic framework MIL-53 (Al) for methylene blue and malachite green dye adsorption, J. Chem. Eng. Data 60 (2015) 3414–3422, doi:10.1021/acs.jced.5b00692.
[38] J.-F. Liu, J.-C. Mu, R.-X. Qin, S.-F. Ji, Pd nanoparticles immobilized on MIL-53(Al) as highly effective bifunctional catalysts for oxidation of liquid methanol to methyl formate, Petrol. Sci. 16 (2019) 901–911, doi:10.1007/s12182-019-0334-6.
[39] E. Rahmani, M. Rahmani, Al-based MIL-53 metal organic framework (MOF) as the new catalyst for Friedel–Crafts alkylation of benzene, Ind. Eng. Chem. Res. 57 (2018) 169–178, doi:10.1021/acs.iecr.7b04206.
[40] P. Rallapalli, K.P. Prasanth, D. Patil, R.S. Somani, R.V. Jasra, H.C. Bajaj, Sorption studies of $CO_2$, $CH_4$, $N_2$, CO, $O_2$ and Ar on nanoporous aluminum terephthalate [MIL-53(Al)], J. Porous Mater. 18 (2011) 205–210, doi:10.1007/s10934-010-9371-7.
[41] III W.P. Mounfield, K.S. Walton, Effect of synthesis solvent on the breathing behavior of MIL-53(Al), J. Colloid Interf. Sci. 447 (2015) 33–39, doi:10.1016/j.jcis.2015.01.027.
[42] X. Qian, B. Yadian, R. Wub, Y. Long, K. Zhou, B. Zhu, Y. Huang, Structure stability of metal-organic framework MIL-53 (Al) in aqueous solutions, Int. J. Hydrog. Energy 38 (2013) 16710–16715, doi:10.1016/j.ijhydene.2013.07.054.

[43] S.-S. Liu, C.-X. Yang, S.-W. Wang, X.-P. Yan, Metal–organic frameworks for reverse-phase high-performance liquid chromatography, Analyst 137 (2012) 816–818, doi:10.1039/C2AN15925B.
[44] L. Alaerts, M. Maes, L. Giebeler, P.A. Jacobs, J.A. Martens, J.F.M. Denayer, C.E.A. Kirschhock, D.E. De Vos, Selective adsorption and separation of ortho-substituted alkylaromatics with the microporous aluminum terephthalate MIL-53, J. Am. Chem. Soc. 130 (2008) 14170–14178, doi:10.1021/ja802761z.
[45] L. Alaerts, C.E.A. Kirschhock, M. Maes, M.A. Van der Veen, V. Finsy, A. Depla, J.A. Martens, G.V. Baron, P.A. Jacobs, J.F.M. Denayer, D.E. De Vos, Selective adsorption and separation of xylene isomers and ethylbenzene with the microporous vanadium(IV) terephthalate MIL-47, Angew. Chem. Int. Ed. 46 (2007) 4293–4297, doi:10.1002/anie.200700056.
[46] Y.-Y. Fu, C.-X. Yang, X.-P. Yan, Metal-organic framework MIL-100(Fe) as the stationary phase for both normal-phase and reverse-phase high performance liquid chromatography, J. Chromatogr. A 1274 (2013) 137–144, doi:10.1016/j.chroma.2012.12.015.
[47] L. Shu, S. Chen, W.-W. Zhao, Y. Bai, X.-C. Ma, X.-X. Li, J.-R. Li, P. Somsundaran, High-performance liquid chromatography separation of phthalate acid esters with a MIL-53(Al)-packed column, J. Sep. Sci. 39 (2016) 3163–3170, doi:10.1002/jssc.201600364.
[48] S. Van der Perre, A. Liekens, B. Bueken, D.E. De Vos, G.V. Baron, J.F.M. Denayer, Separation properties of the MIL-125(Ti) metal-organic framework in high-performance liquid chromatography revealing cis/trans selectivity, J. Chromatogr. A 1469 (2016) 68–76, doi:10.1016/j.chroma.2016.09.057.
[49] W. Qin, M.E. Silvestre, Y. Li, M. Franzreb, High performance liquid chromatography of substituted aromatics with the metal-organic framework MIL-100(Fe): Mechanism analysis and model-based prediction, J. Chromatogr. A 1432 (2016) 84–91, doi:10.1016/j.chroma.2016.01.006.
[50] W.-W. Zhao, C.-Y. Zhang, Z.-G. Yan, L.-P. Bai, X. Wang, H. Huang, Y.-Y. Zhou, Y. Xie, F.-S. Li, J.-R. Li, Separations of substituted benzenes and polycyclic aromatic hydrocarbons using normal- and reverse-phase high performance liquid chromatography with UiO-66 as the stationary phase, J. Chromatogr. A 1370 (2014) 121–128, doi:10.1016/j.chroma.2014.10.036.
[51] S. Chen, X.-X. Li, F. Feng, S. Li, J.-H. Han, Z.-Y. Jia, L. Shu, P. Somsundaran, J.-R. Li, Highly efficient high-performance liquid chromatographic separation of xylene isomers and phthalate acid esters on a homemade DUT-67(Zr) packed column, J. Sep. Sci. 41 (2018) 2528–2535, doi:10.1002/jssc.201800119.
[52] Y.-Y. Fu, C.-X. Yang, X.-P. Yan, Control of the coordination status of the open metal sites in metal–organic frameworks for high performance separation of polar compounds, Langmuir 28 (2012) 6794–6802, doi:10.1021/la300298e.
[53] C.-X. Yang, Y.-J. Chen, H.-F. Wang, X.-P. Yan, High-performance separation of fullerenes on metal–organic framework MIL-101(Cr), Chem. Eur. J. 17 (2011) 11734–11737, doi:10.1002/chem.201101593.
[54] A. Ahmed, N. Hodgson, M. Barrow, R. Clowes, C.M. Robertson, A. Steiner, P. McKeown, D. Bradshaw, P. Myers, H. Zhang, Macroporous metal–organic framework microparticles with improved liquid phase separation, J. Mater. Chem. A 2 (2014) 9085–9090, doi:10.1039/C4TA00138A.
[55] R. Ahmad, A.G. Wong-Foy, A.J. Matzger, Microporous coordination polymers as selective sorbents for liquid chromatography, Langmuir 25 (2009) 11977–11979, doi:10.1021/la902276a.
[56] A. Centrone, E.E. Santiso, T.A. Hatton, Separation of chemical reaction intermediates by metal-organic frameworks, Small 7 (2011) 2356–2364, doi:10.1002/smll.201100098.
[57] M. Maes, F. Vermoortele, L. Alaerts, S. Couck, C.E.A. Kirschhock, J.F.M. Denayer, D.E. De Vos, Separation of styrene and ethylbenzene on metal−organic frameworks: Analogous structures with different adsorption mechanisms, J. Am. Chem. Soc. 132 (2010) 15277–15285, doi:10.1021/ja106142x.
[58] R. El Osta, A. Carlin-Sinclair, N. Guillou, R.I. Walton, F. Vermoortele, M. Maes, D. De Vos, F. Millange, Liquid-phase adsorption and separation of xylene isomers by the flexible porous metal–organic framework MIL-53(Fe), Chem. Mater. 24 (2012) 2781–2791, doi:10.1021/cm301242d.
[59] C.-X. Yang, S.-S. Liu, H.-F. Wang, S.-W. Wang, X.-P. Yan, High-performance liquid chromatographic separation of position isomers using metal-organic framework MIL-53(Al) as the stationary phase, Analyst 137 (2012) 133–139, doi:10.1039/c1an15600d.
[60] S. Van der Perre, T. Duerinck, P. Valvekens, D.E. De Vos, G.V. Baron, J.F.M. Denayer, Chromatographic separation through confinement in nanocages, Micropor. Mesopor. Mat. 189 (2014) 216–221, doi:10.1016/j.micromeso.2013.08.010.
[60] F. Vermoortele, M. Maes, P.Z. Moghadam, M.J. Lennox, F. Ragon, M. Boulhout, S. Biswas, K. G.M. Laurier, I. Beurroies, R. Denoyel, M. Roeffaers, N. Stock, T. Düren, C. Serre, D.E. De Vos, p-Xylene-selective metal–organic frameworks: A case of topology-directed selectivity, J. Am. Chem. Soc. 133 (2011) 18526–18529, doi:10.1021/ja207287h.
[62] F. Yang, C.-X. Yang, X.-P. Yan, Post-synthetic modification of MIL-101(Cr) with pyridine for high-performance liquid chromatographic separation of tocopherols, Talanta 137 (2015) 136–142, doi:10.1016/j.talanta.2015.01.022.
[63] M.A. Moreira, J.C. Santos, A.F.P. Ferreira, J.M. Loureiro, F. Ragon, P. Horcajada, P.G. Yot, C. Serre, A.E. Rodrigues, Toward understanding the influence of ethylbenzene in p-xylene selectivity of the porous titanium amino terephthalate MIL-125(Ti): adsorption equilibrium and separation of xylene isomers, Langmuir 28 (2012) 3494–3502, doi:10.1021/la204969t.